

THESIS

INDIVIDUAL TREE CARBON ESTIMATION RELATED TO GOLD MINE IN BANYUWANGI EAST JAVA

Thesis submitted to the Double Degree M.Sc program of the Gadjah Mada University and
Faculty of Geo-Information Science and Earth Observation of the University of Twente
in partial fulfillment of the requirement for the degree of Master of Science in
Geo-Information for Spatial Planning and Disaster Risk Management



UGM



By:
FITRIANY MADYA ASTUTY
13/357424/PMU/08063
S6013643

Supervisor:
Prof. Dr.rer.nat. Junun Sartohadi, M.Sc
Dr. Y.A. Hussin

GRADUATE SCHOOL
GADJAH MADA UNIVERSITY
FACULTY OF GEO-INFORMATION AND EARTH OBSERVATION
UNIVERSITY OF TWENTE
2015

THESIS

**INDIVIDUAL TREE CARBON ESTIMATION RELATED TO GOLD MINE
IN BANYUWANGI EAST JAVA**

**By:
FITRIANY MADYA ASTUTY
13/357424/PMU/08063
S6013643**

**Has been approved in Yogyakarta
On May 2015**

By Thesis Assessment Board:

Supervisor 1:

ITC Examiner 1:

**Prof. Dr.rer.nat. Junun Sartohadi, M.Sc
Supervisor 2:**

**Prof.dr.V.G. Victor Jetten
ITC Examiner 2:**

Dr. Y.A. Hussin

Ir. Bart Krol

**This thesis has been accepted as one of the requirements
To obtain a Master's degree**

**Program Director of
Geo-information for Spatial
Planning and Disaster Risk Management**

**On behalf of Director
Vice Director for Academic Affairs,
Development and Cooperation**

Prof. Dr. H. A. Sudibyakto, M.S.

Prof. Ir. Suryo Purwono, MA.Sc., Ph.D.

DISCLAIMER

This document describes work undertaken as part of a program of study at the Double Degree International Program of Geo-Information for Spatial Planning and Disaster Risk Management, a Joint Education Program of Institute for Geo-Information Science and Earth Observation, The Netherlands and Gadjah Mada University, Indonesia. All views and opinions expressed therein remain the sole responsibility of the author, and do not necessarily represent those of the institutes.

ABSTRACT

Mount Tumpang Pitu in Banyuwangi East Java is well known as high gold reserves area in Java Island, Indonesia. The existence of small-scale gold mining poses critical concern of forest condition in the area. This study aimed to identify the carbon reserves as indicator of forest degradation due to the presence of gold mining. Remote sensing techniques were used to acquire information for the study objectives. One of the important roles of remote sensing is locating alteration zones. It is the zones of area related to gold deposits.

Landsat-8 OLI images were used to estimate the alteration zone in the study area. The Band Ratio of 4/2-6/5 and Principal Component Analysis can be used to generate ferric iron oxides and ferrous iron oxides mineral reserves. Combining those result with the automated lineament extraction using LINE algorithm resulted estimated alteration zone of gold reserves.

The mining operated as well as the pattern of vegetation cover in the study area can be detected and resulting 14.49 ha of illegal mining area. Meanwhile, estimating the carbon to identify degraded forest was done using Object Based Image Analysis. Result of tree crowns segmentation which has 0.8 of overall accuracy was applied in estimating carbon content of the area. Carbon from trees in small-scale mining was fewer than non-mining area. It had differences of 47.19 ton/ha compares to the area in same alteration zone and 106.04 ton/ha compare to non-alteration zone carbon.

Based on the factor analysis, alteration zone, slope, and parent rock affect carbon reserves. The alteration carbon showed fewer amounts than non- alteration. Slope of the area also affects carbon distribution. Moderate steep slope (15-30 %) gave higher impact of carbon reserves which is contrary to the gentle slope (2-7 %). In terms of parent rocks, sediment clastic became sub-factor that highly influence the carbon reserves.

ACKNOWLEDGEMENT

The success of this study depends on the guidelines of many others. I would like to take this opportunity to express my gratitude to all people who contributed in accomplishing my study.

First of all, I would like to acknowledge Prof. Dr.rer.nat. Junun Sartohadi, M.Sc for his critical ideas, suggestion and patience guidance during the research. Many thanks go to my ITC supervisor Dr. Y.A. Hussin for the support and the assistance to me during the study.

I am very grateful to related parties in MSc Double Degree Program of Geo-Information for Spatial Planning and Disaster Risk Management and all the lectures both of ITC and UGM.

I would like to acknowledge the sponsorship I received from BAPPENAS and NESO who provided me the access to this science experience.

My appreciation goes to Perhutani unit of South Banyuwangi who allows me to conduct the research.

My special thanks to all my classmates for the shared joyful and their support to help each other.

My deepest appreciation is for my family who always loves and supports me during my life. An honorable mention goes to my mother and my father for their unconditional constant love for me.

Lastly, I offer my regards and blessings to all of those who supported me in any respect during the completion of the study.

To my beloved father, this is for you

TABLE OF CONTENTS

DISCLAIMER	i
ABSTRACT.....	ii
ACKNOWLEDGEMENT	iii
TABLE OF CONTENTS.....	v
LIST OF FIGURES	viii
LIST OF TABLES	x
LIST OF APPENDICES	xi
LIST OF ABBREVIATIONS	xii
1. INTRODUCTION	1
1.1 Background	1
1.2 Problem Statement and Justification.....	3
1.3 Objectives	5
1.4 Benefit of the Study	6
2. REVIEW OF RELATED LITERATURE	7
2.1 Geomorphology Unit of Mt. Tumpang Pitu, Banyuwangi	7
2.2 Types of Gold Deposits.....	7
2.3 Hydrothermal alteration	8
2.4 Lineament extraction.....	9
2.5 Forest degradation.....	9
2.6 Carbon stock	11
2.7 Carbon estimation using remote sensing	11
2.8 Object Based Image Analysis (OBIA).....	13
3. STUDY AREA	15
3.1 Geographic location	15
3.2 Topography	16
3.3 Climate.....	17
3.4 Vegetation	17
3.5 Gold reserves	18
4. MATERIALS AND METHODS.....	20

4.1 Materials	20
4.1.1 Imagery data.....	20
4.1.2 Maps and other ancillary data	21
4.1.3 Field instruments.....	21
4.1.4 Software	21
4.2 Methods.....	22
4.2.1 Image processing	24
4.2.1.1 Atmospheric correction.....	24
4.2.1.2. Minimum Noise Fraction	24
4.2.1.3 Band Ratio	24
4.2.1.4 Principal Component Analysis	25
4.2.1.5 Lineament extraction	26
4.2.2 Fieldwork	27
4.2.2.1 Gold mining condition	27
4.2.2.2 Carbon measurement	27
4.2.3 Carbon estimation of airborne imagery	29
4.2.4 Post Fieldwork	34
5. RESULT AND DISCUSSION	35
5.1 Alteration of Landsat 8 OLI.....	35
5.1.1 Atmospheric correction.....	35
5.1.2 Band ratio.....	36
5.1.3 PCA (Principal Component Analysis)	39
5.1.4 Lineament extraction.....	41
5.1.5 Defining alteration zones	44
5.2 Current gold mining ventures	45
5.2.1 Forest cover condition.....	48
5.3 Carbon estimation	49
5.3.1 Descriptive of trees attributes	49
5.3.2 Result of segmentation.....	50
5.3.3 Segmentation accuracy	50
5.3.4 DBH-CPA-Carbon relationship	51

5.3.5 Tree carbon estimation.....	52
5.3.5.1 Total tree carbon	52
5.3.5.2 Tree carbon of small scale gold mining area	52
5.3.6 Analysis factor	54
6. CONCLUSION AND RECOMMENDATION.....	57
6.1 Conclusion	57
6.2 Recommendation	59
LIST OF REFERENCES	60
LIST OF APPENDICES	68

LIST OF FIGURES

Figure 1-1. Mining area of Java and Bali Island 2014	2
Figure 2-1. Placer deposits as the result of hard rocks weathering (“Placer deposit,” 2010).....	8
Figure 2.2 Crown perimeter and crown projection area	13
Figure 3-1. Map of the study area	15
Figure 3-2. Slope of the area.....	16
Figure 3-3. Porphyry deposit on mineralization track of South of Java and Sumbawa (“Geology voice: Potency of gold mineral in Malang Regency (in Indonesia,” 2014)	18
Figure 4-1. Research methodology	23
Figure 4-2. Plot samplings of carbon measurement surrounding illegal mining area.....	27
Figure 4-3. Example of crown density measurement	28
Figure 4-4. Dimension of the plot for biomass (Indonesia Nasional Standard of 7724, 2011)	29
Figure 4-5. Scale estimation of ESP tool.....	30
Figure 4-6. Concept of Multi resolution (Definiens, 2011)	31
Figure 4-7. Hierarchy process in eCognition	31
Figure 4-8. Rule sets of segmentation in eCognition.....	32
Figure 5-1. Atmospheric corrected of 4-3-2 composite band of Landsat-8 OLI	35
Figure 5-2. Spectral reflectance of Iron oxide minerals.....	37
Figure 5-3. Ferric iron oxides distribution	38
Figure 5-4. Ferrous iron oxide minerals distribution.....	38
Figure 5-5. PC1-PC6 images of Principal Component Analysis	40
Figure 5-6. Automatic lineament in <i>PCI Geomatica</i> & rose diagram	42
Figure 5-7. Regional fault system. 1 st order is represented by thick dash lines	43
Figure 5-8. Fault system and river distribution based on the Geology map.....	44

Figure 5-9. Estimated alteration zone.....	45
Figure 5-10. Small-scale mining location	46
Figure 5-11. Mining distribution	49
Figure 5-12. Example of the airborne imagery segmentation	50
Figure 5-13. Distribution of the tree carbon	53

LIST OF TABLES

Table 2-1. Forest degradation assessment (FAO, 2011).....	10
Table 2-2. Advantages and disadvantages of the use of airborne imagery	12
Table 3-1. Temperature and humidity of the area.....	17
Table 3-2. Average precipitation of 2003 – 2010	17
Table 4-1. Instruments used for the data collection	21
Table 4-2. List of the software	21
Table 5-1. The eigenvalue for the MNF bands result	36
Table 5-2. Threshold of the Band ratio 4/2, 6/5, and 6/7	36
Table 5-3. Eigenvalue and eigenvector of Principal Component Analysis result	39
Table 5-5. The Indonesia small scale gold mining category (Aspinall, 2001)	46
Table 5-6. Percentage of forest cover	48
Table 5-7. Descriptive statistic of trees.....	50
Table 5-9. Model of DBH-CPA and CPA-Carbon of trees	51
Table 5-10. Total carbon of the study area	52
Table 5-11. Carbon of the subset area.....	53
Table 5-12. Comparison of area of carbon class.....	54

LIST OF APPENDICES

Appendix 1. The performance characteristic of the Landsat 8 sensor.....	68
Appendix 2. Point of gold mining samples.....	69
Appendix 3. Distribution of mining samples.....	70
Appendix 4. Map of Permanent Sample Plot distribution in Indonesia.....	70
Appendix 5. Sample data collection sheet.....	71
Appendix 6. Accuracy assessment of DBH-CPA model.....	71
Appendix 7. Accuracy assessment of CPA-Carbon model.....	72
Appendix 8. Communalities of analysis factor.....	72
Appendix 9. Teak (<i>Tectona grandis</i> Sp) conformity land criteria.....	73
Appendix 10. Field documentation.....	74

LIST OF ABBREVIATIONS

ASTER	: Advanced Space borne Thermal Emission and Reflection Radiometer
CPA	: Crown Projection Area
DBH	: Diameter at Breast Height
DEM	: Digital Elevation Model
ENVISAT	: Environmental Satellite
ETM	: Enhanced Thematic Mapper
ERS	: European Remote Sensing
FAO	: Food and Agricultural Organization
GIS	: Geographic Information System
GPS	: Global Positioning System
IPCC	: Intergovernmental Panel on Climate Change
MODIS	: Moderate Resolution Imaging Spectroradiometer
MODTRAN	: Moderate Resolution Transmittance
OBIA	: Object Based Image Analysis
OLI	: Operational Land Imagery
RADARSAT	: Radio Detection and Ranging Satellite
REDD	: Reducing Emissions from Deforestation and forest Degradation
RGB	: Red-Green-Blue
RMSE	: Root Mean Square Error
SPOT	: Satellite Pour l'Observation de la Terre / Satellite for Observation of Earth
SWIR	: Short wave Infrared

1. INTRODUCTION

1.1 Background

Mining is the process of obtaining valuable minerals or other geological materials from under the ground. Gold, tin, and coal are some instances of what is extracted from the earth. Gold mining is vital to the economy of many countries whether industrial or developing countries. Gold production provides export revenue, income for the government, and creation of job opportunities. It also brings improvement in physical, social, and financial infrastructure as the essential foundation of economy.

Indonesia produces about four per cent of world's gold production (Indonesia Investments, 2014). High gold reserve is located in some part of Indonesia as reported in the mineral reserves of Geological Agency. As represented in the map of the Decree of Minister of Energy and Mineral Resources (2014), there are some reserves areas especially in Java to mine gold as primary product (Figure 1-1).

Once the location of gold reserves is situated in forest area, it becomes critical concern. Large scale mining which is usually involves company clears the vegetation and use chemicals in extraction process and these are often discharges into streams, rivers or oceans. The small scale is equally devastating for the environment. Land dredging creates pool on the ground, while river dredging caused sedimentation and problems for fish and other living organism. Chupezi, Ingram, & Schure (2009) mentioned sedimentation and contamination of water catchment, loss of biodiversity (deforestation, poaching), number of extinct and threatened species as environmental impacts of mining.

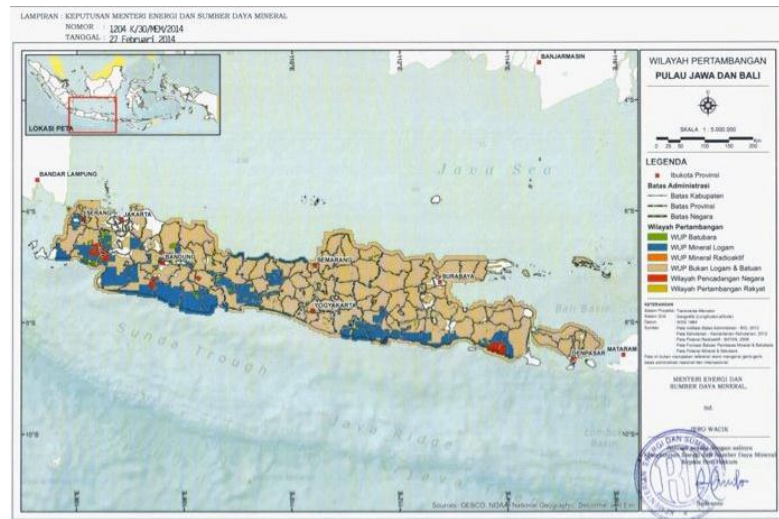


Figure 1-1. Mining area of Java and Bali Island 2014

Small-scale gold mining phenomenon in Banyuwangi East Java poses decreasing in river condition, which is Gonggo River, becomes wider and deeper. Damage to the Teak plantation is also one of the results of the existence of mining ventures (Energy and Mineral Resources Departement, 2009). As the driving factor to the environmental degradation, it is essential to identify where, why, and at what level is the impact of gold mining (CPF, 2014). FAO (2003) stated that assessment requires actual condition knowledge and the changes at appropriate levels. Inevitably, with the advance of remote sensing and geographic information systems nowadays, it can perceive this assessment. Remote sensing has the capability to acquire information both spatial and temporal of environmental parameters that are not available from in situ measurements. There has been phenomenal growth in the field of satellite remote sensing over the last two decades (Woldai, 2001). By analyzing satellite imageries, gold mining impact is possible to identify.

1.2 Problem Statement and Justification

According to Woldai (2001), mining involves several stages namely site development, mining, mineral extraction, and mine closure. Each phase has potential of different impacts depending on the local terrain, the type of technology, and ability to monitor and compliance with regulations. Initiating access in site development disturbs vegetation, wildlife, and consequently deforests the area. Whether surface or underground mining, it requires land for waste rock disposal, storage of ore and raw material, and siting of facilities. While in situ mining which is involving toxic injection to the earth represents least environmentally positive aspect as well as mineral processing which involves chemically intensive activities. Each mining activity is different from others. Therefore, mining activities vary in terms of its impact on the environment and consequently would need different mapping approach.

The activities of mining in forest area influences vegetation cover. It poses loss of the vegetation properties for other purposes. Contaminations of surface and ground water bodies also become significant environmental destruction (Tom-Dery, Dagben, & Cobbina, 2012). Mining involves the clearing of forest and it is leading to serious forest degradation.

Forest degradation is the capacity decreasing to provide good and services of forest (FAO, 2011). It is including degraded primary forest, secondary forest, or degraded forest land. Degraded forest land is including the disturbances or land uses that damage soil and vegetation to a degree that inhibits or severely delays the re-establishment of forest after abandonment. Database regarding the mine, mine operation, and its impacts on the ecosystem is not available (Woldai, 2001). Integration of the information is required in order to arrive at environmental impact assessment. In addition, this might serve as basis for the decision makers to support the sustainable forest management.

Referring to the advantage of satellite based remote sensing data; it is a promising technique to recognize the degradation of forest cover due to gold mining

activities. In addition, the study about utilization of satellite based remote sensing to detect degraded forest in Indonesia due to mineral resources exploitation indicates under application. Therefore, it becomes important to gather this kind of information with cost-effective and within short period of time. Since the extent of mining area has grown rapidly, new challenge to gather landscape impact is performed.

The sensor that used to detect the mining also varies which is ranged from optical to radar sensor. Woldai & Fabbri (1998) used black and white aerial photographs from 1973 to assess the existence of new dumpsite/barren area. ASTER imagery combined with IKONOS successes in characterizing and mapping mining residues area such as tailings and waste piles (Chevrel, et al., 2005). In addition, radar sensor was used partly for monitoring mine subsidence in South west of Sidney by using ERS1, JER 1, RADARSAT-1, and ENVISAT (Ge, Chang, & Rizos, 2007).

Remote sensing image processing to generate mining information also differs which is started with manual interpretation. For instance, conventional image differencing method using visual and on screen digitizing to assess environmental pollution over the central Kola Peninsula studied by Rigina in 2002. Intensity Hue Saturation (IHS) transformation as a technique to enhance image has been used in the transformation of SPOT panchromatic with ASTER multispectral data (Charou, et al., 2010). It can identify land cover classes in mining area. Furthermore, Gao, et al. (2003) classified the Moderate Resolution Imaging Spectroradiometer (MODIS) using object based image analysis technique with satisfy classification.

One of the important roles of remote sensing is locating alteration zones that related to gold deposits. Band rationing, Principal Component Analysis (PCA) and other methods have been developed to extract alteration zones. Gabr, Ghulam, & Kusky (2010) detected hydrothermal alteration zones for gold exploration using ASTER images in Egypt. The processed Landsat ETM+ and ground investigation

were used to indicate three main gold-bearing shear zones in NW Nigeria (Ramadan & Abdel Fattah, 2010).

This study addresses the use of imagery for recognizing alteration zones and deforested area caused by extracting gold activities. To produce a map of degraded areas, images had been interpreted by identifying the forest cover and carbon stocks condition. As the increasing of mining pressure to the forest, spatial variability in carbon stocks is ought to understand since deforestation immediately releases the carbon (Shrestha, 2011). It is due to one of the efforts to mitigate climate change through the Reduced Emissions from Deforestation and Degradation (REDD) by mapping tropical forest carbon.

1.3 Objectives

The main objective of the research is to identify and to detect gold mining ventures and carbon stock estimation lost as the consequences of deforestation condition using remote sensing imageries. As database, spatial extent of mining within forest generates information to assess environmental impacts. Specifically, the research addresses following sub-objectives:

1. To identify the gold alteration zones distribution using remote sensing imageries
 - 1.1 What are the proper techniques required to generate alteration zones
2. To estimate the trees carbon of the gold alteration zones
 - 2.1 How much the difference of carbon content between alteration and non-alteration zones?
3. To identify and detect a small-scale gold mining setup using high resolution airborne multispectral imagery
 - 3.1 How accurately can a gold mining and its spatial pattern detected in the study area?
 - 3.2 What is the condition of vegetation cover and its pattern in an area of gold mining?

- 3.3 How accurately can carbon stock lost to degradation because of gold mining be estimated and mapped using high-resolution airborne multispectral imagery and OBIA
- 3.4 How much carbon stocks have been lost for forest degradation because of mining activities in small-scale gold mining area
- 4. To recognize the factors that influence carbon distribution
 - 4.1 What are the factors that influence the carbon distribution

1.4 Benefit of the Study

The benefits of the research hopefully can be used by the local government and many stakeholders that have interest in gold mining and its effect on forest management, such as:

- 1. It performs the situation of mining, especially information of environmental degradation that can be used as a valuable input to minimize the risk.
- 2. It may represent in policy recommendation to local government to overcome the problem of small-scale mines.

2. REVIEW OF RELATED LITERATURE

2.1 Geomorphology Unit of Mt. Tumpang Pitu, Banyuwangi

According to Sartohadi et al., (2014), Mt. Tumpang Pitu is situated in the southern part of Ijen volcano. In the end of the Tersier era, the sediment of Tersier Ijen volcano uplifted on the sea level in line with the andesite-diorytic intrusion. It formed relatively coarse relief of geomorphology unit which is known as Batu Ampar formation. Based on the geology map, the parent rocks of the area are dominated by sediment-clastic- sands and intrusive felsic.

The part experiencing intrusion andesite-diorytic has a relatively thick surface. The surface becomes fragile and weathered intensively on its underside because of depressed and impelled by the hot-intrusion rocks. The layer of the surface cover start is material of rock intrusion andesite-diorytic at the bottom, weathered material from the surface to direct contact with rock intrusion, the massive surface rocks, and the weathered-rock surface at the very top.

The motion process of the intrusion mass has relatively greater magnitude. This large dimensional motion is caused by weathered material due to direct contact with hot-intrusion rock. The minute weathered material saturated by water, it leads to become unstable and easily moved down the slopes above of intrusion andesite-diorytic massive rocks. The process will bring all the small material as well as massive rocks (Sartohadi et al., 2014).

2.2 Types of Gold Deposits

Gold is frequently shaped within the magma underneath the crust of the earth (Najafi, 2011). Many miners find gold as deposits in rivers, which come from the ore that are washed out due to wind and erosion (Figure 2-1). Stream placer happens when water carries gold along with other minerals and stones far from the hard rock deposits. As the velocity of water declines, heavier minerals are

dropped before the lighter ones. Alluvial deposits occur when the deposits are already located on a hilltop as wind and water erode finer sediment.

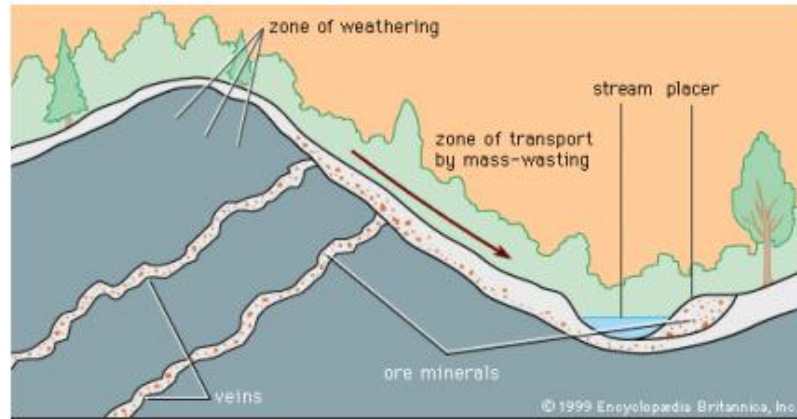


Figure 2-1. Placer deposits as the result of hard rocks weathering (“Placer deposit,” 2010)

2.3 Hydrothermal alteration

Hydrothermal system drives by magmatic intrusion in the upper crust (Hedenquist & Lowenstern, 1994). The hydrothermal fluids alter the chemical composition within the rock. Different igneous rocks produce various minerals. As the water heated by hot magma, it alters the rocks and poses the solutions become mineral rich. This mineral rich solution moves following the fractures or cracks. Veins are created once the solutions are cooled in the rock fractures (Patterson, 2003). Recognizing minerals distribution of the alteration zone is useful for discovering the metal elements deposits (Shanks III, 2012).

Alteration widely studied using remote sensing data. Amin Beirandvand Pour & Hashim (2014) presented the using of Landsat-8 for hydrothermal alteration of porphyry copper in arid and semi-arid area. Gabr et al. (2010) used ASTER to mapping the gold mineralization and tested a new method to identify alteration zone.

2.4 Lineament extraction

A lineament is any extensive linear surface as a fault line or fracture line (Abdullah, Nassr, & Ghaleeb, 2013). Lineaments could be straight streams and valleys, topographic alterations, natural vegetation alignment and height changing. Either by visual or automatic extraction, it is a valuable information of structural setting. Many studies of linear geologic setting have been progressing. Kocal et al. found that automatic extraction yields effective result in high-resolution image. Meanwhile in semi-arid area, Abdullah, Nassr, & Ghaleeb (2013) concluded that Landsat ETM-7 was powerful in lineament analysis.

In terms of tropical area, the using of optical remote sensing image in defining lineament has boundaries related to the dense vegetation and man-made features (Hashim, et.al, 2013) . To overcome these problems, the use of DEM (Digital Elevation Model) was selected. Automatic lineament is based on the edge enhancement followed by sharpening of the most appropriate band. Automatic delineation can extract from small to large scale of lineaments and resulting trend analysis of the direction.

2.5 Forest degradation

Forest degradation is the capacity of decreasing forest cover to provide good and services of forest (FAO, 2011). It is including degraded primary forest, secondary forest, or degraded forestland. Degraded forestland is including the disturbances or land uses that damage soil and vegetation to a degree that inhibits or severely delays the re-establishment of forest after abandonment.

There is no patent indicator to assess forest degradation. Indicators listed by one or more countries such as disappearance of biodiversity or species, erosion, forest cover, water quality, soil fertility, soil structure, soil properties, wildlife habitats, and wildlife risk.

Table 2-1. Forest degradation assessment (FAO, 2011)

(d): Local and Field/Farm levels

Systems assessed	Methods used	What was assessed	Units / values
Lands (cropland lands, grasslands, forests, conserved area, deserts etc.), Soils, Rivers, Rangelands, etc.	Expert opinion (e.g. indicators, questionnaires, interviews, focus groups, etc.) Land users opinion (e.g. indicators etc.) Remote Sensing and GIS (e.g. NDVI, MODIS, MSDI ect.) Modelling (e.g USLE/ RUSLE, CORINE, PESERA models, etc.) Field monitoring and measurements (verify models) - farm plots Estimates of productivity changes	Land/soil degradation: - severity, degree, extent, impact, causes, & risks,, Soil erosion (Sediment yields)	%, Classes (1,2,3,4,5 for light – very severe; extremely health – extremely unhealthy, etc.),
		Rangelands Health/ condition Soil condition (quality, salinity, stability, fertility, etc.), Crop yield & suitability, Soil condition, Landscape/ ecosystem function, Land cover, Biodiversity loss, Land uses, Climate (rainfall, temperature), etc.	t/ha/yr Frequency of indicators

The extent of degradation could be measured based on the estimated percentage loss of good or services. For instance, a forest that is producing 20 per cent less wood than in the past or population of given species is 30 per cent below minimum baseline level. Over time indicators measurement shows that degradation is occurring.

The concerns of deforestation due to mining are diverse with various environmental consequences. It has steered to the loss of forest products, flooding, erosion, pollution, high degree of siltation of streams, decline of biological diversity and speeding up of extinction of flora and fauna, increase in carbon dioxide and temperature of the atmosphere, increase rate of evaporation and alteration of fluvial competence and capacity (Mustafa, 2010).

FAO (2011) stated that the use of canopy-cover percentage as indicator can be used to provide degradation information. It can associate with a biomass of growing stocks or carbon stored. Combining permanent sample plot in forest with a remote sensing technique has relatively moderate cost to assess biomass or carbon calculation.

2.6 Carbon stock

Decreasing of the carbon stock addresses one of the statuses of forest degradation. Tropical forests have major part in mitigating climate change by sequestering carbon. What time cleared or degraded forest contributes one-sixth of global carbon emissions (FAO, 2011). Avoiding and reversing tropical deforestation is a potentially least-cost response to mitigating climate change.

Biomass is the total quantity of live organic matter and inert organic matter (IOM) aboveground and belowground expressed in tons of dry matter per unit area. Typically, the terms of measurement are density of biomass expressed as mass per unit area, e.g. tons per hectare. The total biomass for a region is obtained by aggregating of the density of the biomass at the minimum area measured.

Carbon estimation requires detailed estimations of biomass of all land cover types. According to the IPCC (2006), above ground biomass including biomass of living vegetation, both woody and herbaceous, above the ground including stems, stumps, branches, barks, seeds and foliage. Mandal (2012) found that plant stages contribute diverse involvement in carbon stock. Trees and poles offer higher contribution than saplings and seeds. Brown (1997) stated above ground biomass of trees is the greatest element of total living biomass in a forest. Understory is about 3 per cent, dead wood 5-40 per cent, and fine litters 5 per cent of above ground tree biomass. Hence, measuring AGB can be readily converted to carbon stock which is fundamental in understanding carbon cycle.

2.7 Carbon estimation using remote sensing

IPCC (2006) mentioned estimation of biomass can be obtained using remote-sensing images through some ways: (i) generating a vegetation type map; (ii) estimating using some quantitative relationship (e.g. regression equations); (iii) Stratifying the vegetation as a sampling framework of fieldworks.

Remote sensing and its developments has become a popular technique to monitor forest ecosystem and its service (Erk, 2011). High spatial resolution of airborne imagery has been used for wide applications such as forest inventory (Nguyen, 2010). Various parameters such as diameter of the crown, crown closure and standing stock can be derived from airborne photographs. Yet, the airborne imagery has both advantages and disadvantages summarized in Table 2-2.

Table 2-2. Advantages and disadvantages of the use of airborne imagery

Advantages	<ul style="list-style-type: none"> • Covers large area at the same scale of the land • High resolution • Better stereoscopic interpretation • Reach inaccessible area • Possible to measurement in known scale
Disadvantages	<ul style="list-style-type: none"> • Relief displacement • Highly cost • Longtime acquaintance

Estimating carbon from the field can be done by measuring DBH (diameter at the breast height) alone or in combination with tree height which is resulting relationships (allometric equation). In remote sensing, the estimation requires the statistical relationship between tree parameters and field measurement (Gibbs, et al., 2007). Furthermore, it needs to develop the biomass predictive models and its validation of the forest characteristics.

Since carbon stock cannot be directly generated from the imagery, allometric equation can link the carbon with the parameters. Tree allometry is the use of equations to describe relationship of various tree parameters. Estimation of carbon for individual trees (ton per hectare) is obtained by dividing total carbon by the sample area. Uncertainty of error should be minimized in order to minimize the overall error.

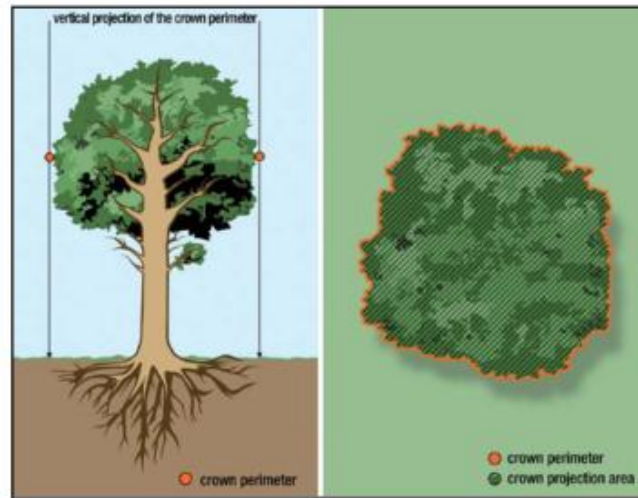


Figure 2.2 Crown perimeter and crown projection area

The relation between DBH (Diameter at Breast Height) and CPA (Crown Projection Area) can be applied to estimate carbon stock. CPA is vertical projection of the tree crown on the horizontal plane (Figure 2-2). The study by Wardani (2013) showed the relation of DBH-CPA-above ground carbon of broadleaves and pine trees in Merapi National Park. Shrestha (2011) concluded that there were relationships between fields DBH and segmented CPA of needle leaved and broadleaved trees resulted from GeoEye satellite image.

2.8 Object Based Image Analysis (OBIA)

Blaschke, et al. (2002) stated that most methods to classify object is based on the statistical property of the image such as spectral reflectance. The question is how if several spectral bands are included or there are no readily available boundaries. In many cases, the meaningful object creates when image is segmented in homogenous area. It purposes to aggregate data in order to minimize the variation within the object and minimize the classification error (Lee & Warner, 2014).

Object based image analysis (OBIA) analyses the image based on its objects instead of its pixel. An object is defined as a group of pixels with similar spatial and spectral properties. Some criteria such as scale, color, smoothness, and

compactness define the segmentation to get meaningful objects. Homogeneity of spectral, spatial, contextual, and textural characteristics is also applied in object oriented. Two basics approaches in segmentation are top-down (cutting something big into smaller part) or bottom-up (merging small parts to obtain bigger object).

Some studies had been conducted in applying OBIA in terms of forestry application. Karna (2012) applied multi-resolution segmentation on Worldview-2 to estimate above ground carbon stock. Shrestha (2011) also segmented individual crown based on the object based analysis in some forest of Nepal. In 2013, Wardani studied above ground carbon stock change by applying OBIA to obtain crown projection area of the trees in Merapi Volcano National Park.

3. STUDY AREA

3.1 Geographic location

Mount Tumpang Pitu is situated in the east part of the island of Java, regency of Banyuwangi (Figure 3-1). Administratively, Banyuwangi is divided into twenty four sub districts and the study area is located in Pesanggaran sub district. Geographically, the study area is lied between $8^{\circ}58' - 8^{\circ} 63'S$ and $114^{\circ}03' - 114^{\circ}08' E$, with area of 2101.89 hectares.

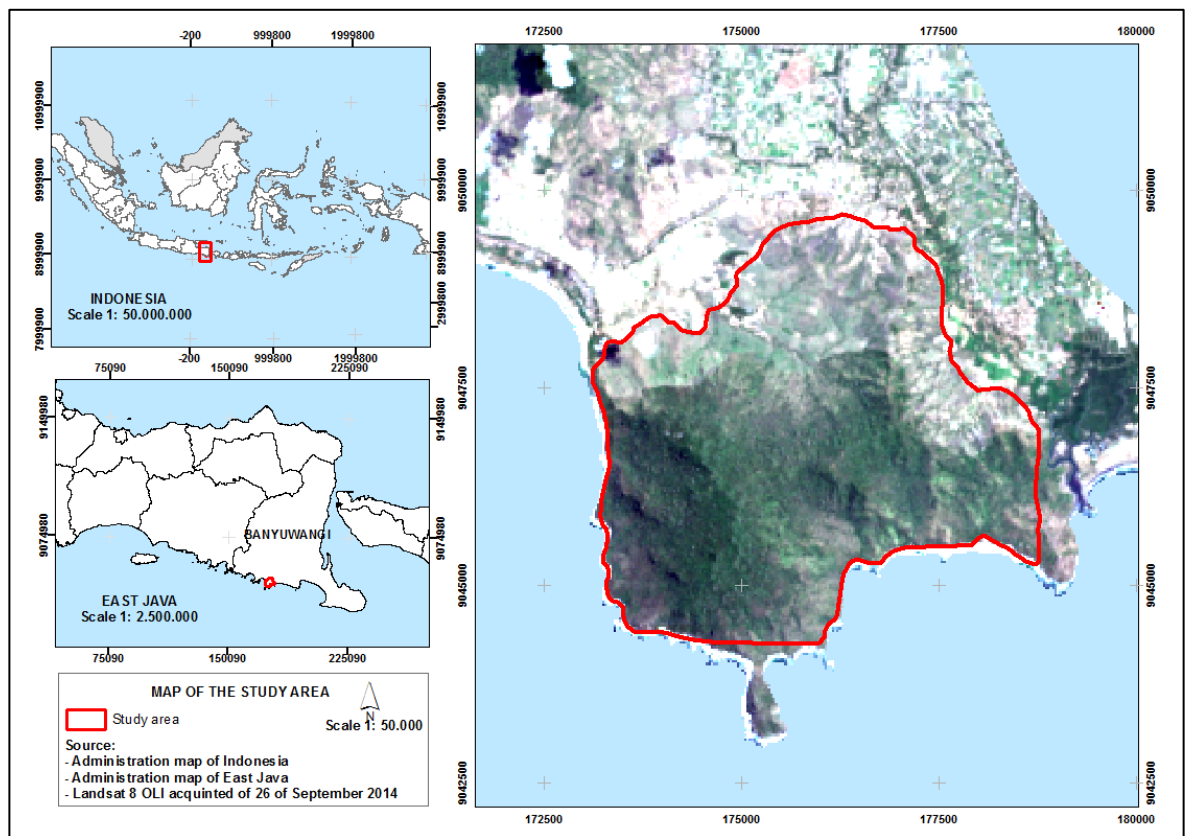


Figure 3-1. Map of the study area

3.2 Topography

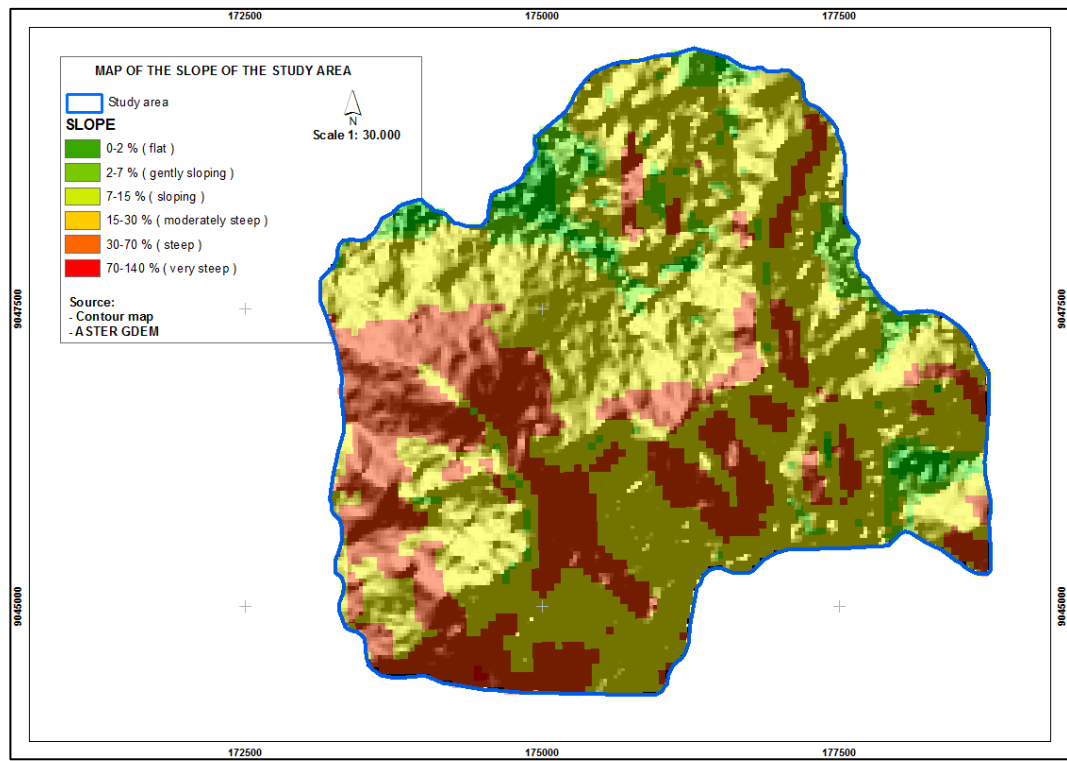


Figure 3-2. Slope of the area

Topography of the area is characterized by various slopes from flat to steep slope with range of elevation between 0 and 1000 meters above sea level (Figure 3-2). The slopes mostly are steep and moderate steep, some from sloping to flat. However, some areas in the southern and western part have steeper slopes.

Based on the geology map, the study area consists of latosol and litosol soil type. Latosol is type of soil which had further weathering with low content of organic material and primary mineral and low pH (4.5-5.5) (Center of Soil Research, 1982). Meanwhile, litosol has shallow depth that lies on the hard rock and has profile as a result of erosion process. Typically, this type of soil is found in an area with steep slope.

3.3 Climate

It has a typical tropical climate with high temperature, humidity and precipitation. Average rainfall in the area is 1934 mm and most of the rainfalls occur during November – March. The monthly average of temperature and relative humidity is presented in Table 3-1. Meanwhile, for the average precipitation of the area from 2003 to 2010 is summarized in Table 3-2.

Table 3-1. Temperature and humidity of the area

Month	Temperature (°C)	Humidity	Month	Temperature (°C)	Humidity
Jan	26.7	86	July	26.1	82
Feb	27.7	81	Aug	26	78
March	27.4	82	Sept	26.3	77
April	24.8	83	Oct	28.2	75
May	27.5	84	Nov	27.4	82
June	27	86	Dec	27.2	83

Table 3-2. Average precipitation of 2003 – 2010

Month	Precipitation (mm)	Rainy day	Month	Precipitation (mm)	Rainy day
Jan	321.5	15	July	27.6	3
Feb	329	14	Aug	2.1	1
March	296.1	15	Sept	63.5	4
April	120.2	7	Oct	40.3	3
May	81.2	5	Nov	229.4	10
June	41.6	4	Dec	382.1	16

Source: Climatology, Meteorology and Geophysics Agency of Banyuwangi (2014)

3.4 Vegetation

The vegetation cover of some area is Teak *Tectona grandis* plantation of 2002 planting year. The other species found in the study area are *Artocarpus elasticus* and *Bishofia javanica*. Some part of the research area belongs to plot of 78 and plot of 79 of Perhutani as the authority who manage the Teak production forest in Java Island. All of those species given above, having oval or rounder shaped crowns, are called as broadleaves trees.

The distance planting used in Teak plantation is 3 x 3 m (1111 trees per hectare). Thinning is applied every three years for plant of 3 to 15 years. It is followed by every 5 years thinning until 30 years and every 10 years thinning of plantation of more than 30 years. Thinning is done by selective cutting of about 7 % of total number of trees. Meanwhile, Clear cutting is done in 60 years.

3.5 Gold reserves

Geologically, south part of Java Island is formed as a consequence of the ancient volcano. In addition to fertilize land, this ancient volcano also produces metallic mineral deposits of gold, silver and copper. Along the southern strip of Java Island a variety of gold mines are found which are economical among other such as: Cibaliung (Banten), Cikotok (Sukabumi), Pongkor (Bogor), Ciemas (Sukabumi) and Tumpang Pitu (Banyuwangi).

According to Van Bemmelen cited in “Geology voice: Potency of gold mineral in Malang Regency (in Indonesia),” (2014), the south part of Java Island is called by Old Andesite formation. This is due to most of southern java is formed by ancient volcanic that produces rock with a composition of andesitic (Figure 3-3).

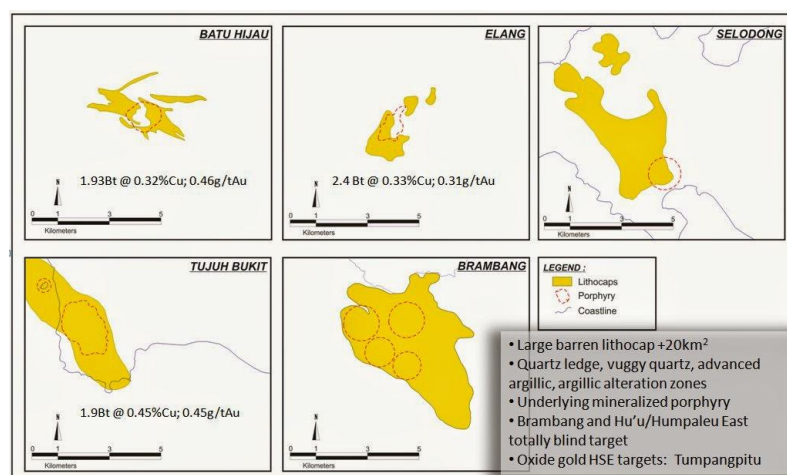


Figure 3-3. Porphyry deposit on mineralization track of South of Java and Sumbawa (“Geology voice: Potency of gold mineral in Malang Regency (in Indonesia,” 2014)

The potential distribution of primer gold was discovered in the form of quartz in the sinews of volcanic rock that breached by intrusive igneous rock of diorite, andesite, granodiorite and dacite. Based on a feasibility study (Energy and Mineral Resources Agency, 2013), ore of primer gold deposits reached 1.700.000.000 tons with the average levels of gold reach 2.3 grams per ton. Besides primary gold reserves found, there are also secondary gold around the primary gold. The existence of this secondary gold mostly within the domain of Perhutani land, that their distributions follow old rivers. It is contrary to the fact that according to the spatial planning of East Java 2020 (Communication and Information Agency, 2009), Mt. Tumpang Pitu has been set as a high categories water catchment area, 30 liters per second.

4. MATERIALS AND METHODS

4.1 Materials

4.1.1 Imagery data

Landsat-8 Operational Land Imagery (OLI) images were obtained from USGS Earth Resources Observation and Science (EROS) Center Archive (<http://earthexplorer.usgs.gov/>). The Landsat 8 OLI sensor launched on the 11th of February 2013 has a 16-day temporal resolution. On board the Landsat 8 OLI sensor has two instruments: (i) the Operational Land Image (OLI) and (ii) the Thermal Infrared Sensors (TIRS). Landsat-8 image has 11 bands; 5 in the visible and Near-Infrared (VNIR), 2 in the Thermal Infrared (TIR) region of the electromagnetic spectrum, 2 in the SWIR region, 1 in Pan Region and 1 panchromatic channel (band 8). Spatial resolution is 15 m for the panchromatic band, 30 m for VNIR and SWIR bands, and 100 m for the TIR bands. Two additional bands represent the different between Landsat 8 and the previous product (Landsat ETM+), a deep blue coastal / aerosol band and a shortwave-infrared cirrus band (Appendix 1). In this research the bands that used was band 1-7 as multispectral image. The image which has been used in this study was captured on 26th of September 2014.

The airborne imagery used for the analysis in this research was collected on 11th of November 2013, has resolution of 0.15 m and has only three spectral bands which are blue (450-510 nm), green (510-580 nm), and red (655-690 nm).

The ASTER GDEM data of the area was downloaded from gdem.ersdac.jspacesystem.or.jp. Advanced Spaceborne Thermal Emission and Reflection Radiometer Global Digital Elevation Model Version 2 (ASTER GDEM V2) released on October 17, 2011, maintains the GeoTIFF format with 30-meter postings.

4.1.2 Maps and other ancillary data

Digital base map and contour map published by the Ministry of Forestry were used in this research. Similarly, land cover map and administration boundary map were also used. In addition, the geology maps scale of 1:100.000 published by Energy and Mineral Resources was used in analysis.

4.1.3 Field instruments

Various field equipment were used to collect the field data. A detail of the instruments is given in Table 4-1.

Table 4-1. Instruments used for the data collection

No	Instruments	Function
1.	Garmin GPSmap 60CSX	navigation and positioning
2.	Diameter tape	measuring the tree diameter
3.	Haga hypsometer	measurement of tree height
3.	Surveyor tape, compass	creating the sampling plot
4.	Camera	documentation

4.1.4 Software

Different software were used for the analysis of imageries data during pre and post fieldwork. Table 4-2 shows the specific use of software.

Table 4-2. List of the software

No	Software	Function
1.	ENVI 5.1	Image processing and registration
2.	Arc GIS 10.2	GIS analysis
3.	PCI Geomatica 2014	Image analysis
4.	Ilwis 3.3	Image analysis
5.	eCognition Developer 8.7	tree crown segmentation
6.	MS office 2010	Data analysis and thesis writing

4.2 Methods

The method of the research mainly comprises of three parts: image processing, fieldwork for data collection, and carbon estimation. Atmospheric corrected Landsat image was further processed to obtain alteration zone. Estimating carbon using segmentation of CPA (Crown Projection Area) was done in eCognition program. By defining the gold alteration zone and carbon potential of the area, the relation of both variables could be attained. A flow diagram showing the research methodology is illustrated in Figure 4-1.

The purpose of mapping the alteration zone using Landsat-8 OLI is to gain the difference of individual tree carbon stock. As the possibility of mines venture is located in the area with high gold reserves, the canopy structure will be more distressed than undisturbed forest. It leads to the decreasing of the amount of the trees biomass as well as its stored carbon. As the study of Alvarez-Berríos & Mitchell Aide (2015), the gold mining sites losses forest cover in tropical moist forest of South America. Lowe (2014) also stated that 2009 deforestation in Guyana attributed to mining showed high increase in forest removed. Despite to achieve the objective of this study, the writer realize that technique used in defining mineral alteration zoning cannot be properly used by the Geologist to delineate the gold minerals distribution in the study area.

All of the digital data were processed using UTM (Universal Transverse Mercator) zone 50S map projection and the WGS (World Geographical System) 1984 coordinate system.

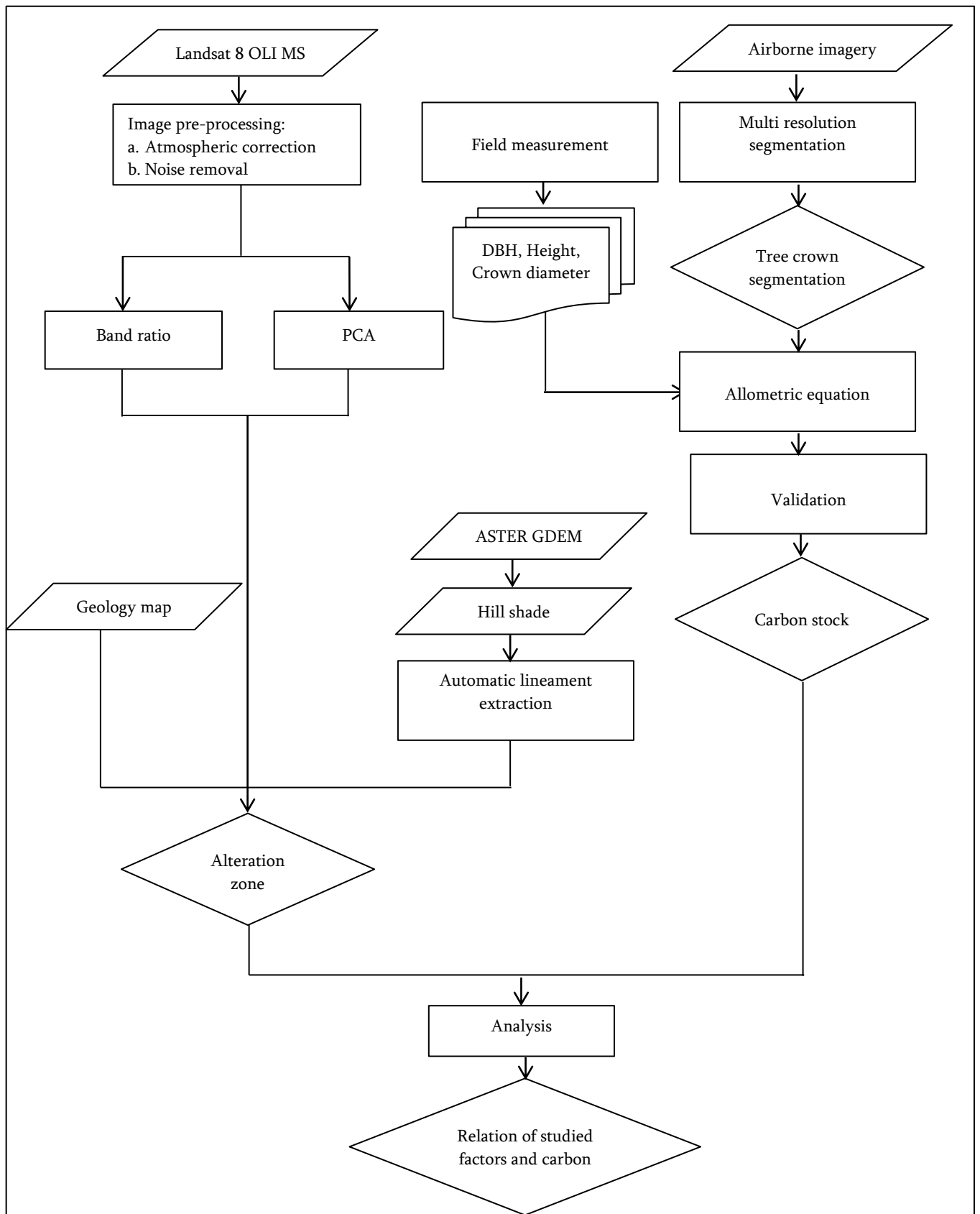


Figure 4-1. Research methodology

4.2.1 Image processing

4.2.1.1 Atmospheric correction

To overcome dark appearance of Landsat-8 OLI, it was atmospheric corrected using FLAASH (Fast Line-of-sight Atmospheric Analysis of Spectral Hypercube) method. It is a first-principles atmospheric correction tool that corrects wavelengths in the visible through near-infrared and shortwave infrared regions, up to 3 μm (IDL, 2009). Based on the study of Perkins et al. (2005), FLAASH is capable of generating accurate surface reflectance spectra from multi spectral image data. Condition of clear to moderate aerosol/haze, low to moderate water vapor, and nadir viewing from any altitude between the ground and the top of the atmosphere can improve the accuracy using FLAASH. FLAASH incorporates with the MODTRAN[®] radiate transform algorithm (Berk et al., 1998). It uses to correct wavelengths of visible, near infrared and sort-wave infrared range.

4.2.1.2. Minimum Noise Fraction

The Minimum Noise Fraction (MNF) transform is an algorithm to determine the inherent dimensionality, to separate noise, and to reduce the computational requirements for processing of the image (ITT Visual Information Solutions, n.d.). MNF consists of two principal transformations. First, based on the noise covariance matrix decorrelates and rescale the noise. Second transformation is by examining the eigenvalues and associated images. This technique was used to identify altered rocks by density slice technique. Ali & Pour (2014) used MNF to identify hydrothermally altered rocks in Ariab mining district, Sudan.

4.2.1.3 Band Ratio

Following the pre-processing of the images, Band Ratio has been used in determining lithological and alteration zones. The technique distributes the

brightness values at tops and creates a reflectance curve (Ali & Pour, 2014). It used in highlighting materials such as minerals. Pour & Hashim (2014), who studied Landsat ETM+ to mapping alteration mineral in Sarawak Malaysia, used several band ratios to generate further analysis of suppressing effects of vegetation and tropical terrain. They used band ratio 4/2 (the equivalent to band ratio 3/1 of Landsat ETM+) and 6/7 (the equivalent to band ratio 5/7 of Landsat ETM+). In addition, Ali & Pour (2014) used the combination of Sabin's ratio RGB images (4/2-6/5-6/7) to obtain alteration zones. The applied Sabins's ratio (Sabins, 1999) to atmospheric corrected Landsat-8 OLI resulted qualitative detection of alteration mineral in the study area. The ratio 4/2 highlights ferric iron oxides that absorbs blue and highly reflects red. The 6/5 ratio highly reflects ferrous iron oxides minerals. Iron oxide highly reflects in the range of 0.63-0.69 μm , while vegetation reflects highly in 0.7-0.9 μm (NIR range). It causes iron oxide can be distinguish from vegetation. The 6/7 ratio is capable in mapping kaolinite, montmorillonite and clay minerals (Ali & Pour, 2014). Band 7 of Landsat 8 OLI in SWIR region absorbs rock features due to composition of Al-Oh, Fe, Mg-Oh, Si-O-H and CO₃ (Pour & Hashim, 2014).

4.2.1.4 Principal Component Analysis

Reducing dimensionality of the correlated multispectral data is the objective of the Principal Component Analysis (Bodruddoza Mia & Fujimitsu, 2012). PCA has been used widely to identify lithological units (Gabr et al., 2010; Liu et al., 2013; Ali & Pour, 2014). Uncorrelated linear combinations (eigenvector) with smaller variance are selected. The variance is related to spectral response of various surface materials and statistical dimensionality of the data. Eigen values give information of spectral properties related to statistical variance of each Principal Component.

4.2.1.5 Lineament extraction

Lineament as one of the geological features can be generated from the topographic or remote sensing images. The usage of hill shade DEM generated from the ASTER GDEM would help the extrapolation of lineament. Sukamar et al. (2014) studied automatic extraction using edge-detection algorithm built in PCI Geomatica to extract the lineament.

Kocal et al. mentioned three stages of LINE algorithm. Firstly, Canny edge detection is used to strength the edge of the image. Gaussian filter with RADI (Radius of filter in pixels), gradient computation, and suppression of the gradient are applied in the Canny algorithm. Secondly, GTHR (threshold for edge gradient) is used as threshold to get a binary image from the edge strengthen image. Thirdly, binary image generates curves. This step consists of several steps; (i) applying the thinning algorithm to the binary edge image in order to produce pixel-wide skeleton curves; (ii) extracting a sequence of pixels for each curve from the image; (iii) discarding any curve with the number of pixels less than the LTHR (threshold for curve length) parameter value, (iv) converting an extracted pixel curve to vector form by fitting piecewise line segments; (v) The resulting polyline is an approximation to the original pixel curve where the maximum fitting error (distance between the two) is specified by the FTHR (threshold for line fitting error) parameter; (vi) the algorithm links pairs of polylines which have criteria: two polylines face each other and have similar orientation (the angle between the two segment is less than the parameter ATHR- threshold for angular difference; the two end-segments are close to each other (the distance between the end points is less than the parameter DTHR- threshold for linking distance).

4.2.2 Fieldwork

4.2.2.1 Gold mining condition

Condition of gold mining impact in the study area is obtained by observation and interview with the miners. The purpose of interview was to get detailed information about mining activity. On the other hand, to check the truth of visual interpretation of gold mining ventures, the 30 number of mining point samples were used (Appendix 2). The point location of gold mining is divided into two types, underground and along the river mining.

4.2.2.2 Carbon measurement

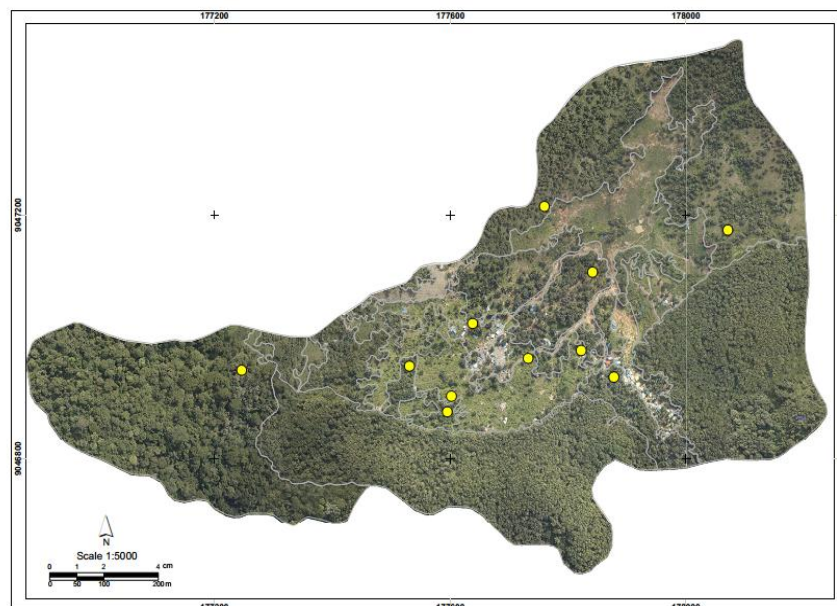


Figure 4-2. Plot samplings of carbon measurement surrounding illegal mining area

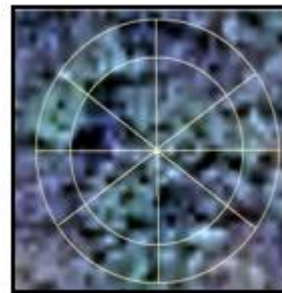
Based on the Indonesia Nasional Standard of 7724 (2011), sampling technique that can be used in carbon measurement are stratified systematic sampling or simple random sampling. However, in order to get representative of all classes, this fieldwork was done by stratifying the crown density of the standing stock at

the first. Number of the sample units that used was eleven plots by considering that the area is dominated by Teak forest plantation (Figure 4-2). Classification is applied by manually interpreting the airborne imagery. The class distribution is based on the *crown density (C)*. Determination of crown density classification according to (Jaya, 2006), namely:

- C1 for crown density 10-30 %
- C2 for crown density 31-50 %
- C3 for crown density 51-70 %
- C4 for crown density 71-100 %



C1 (25%)



C4 (87.5%)

Figure 4-3. Example of crown density measurement

Meanwhile, the data that represents the rest of the study area was obtained from the permanent sample plot. Permanent sample plot (PSP) is used in National Forest Inventory to acquire forest resources data (Appendix 4). The PSP fixed plot has dimensional of 100 m x 100 m which is divided by 25 m x 25 m unit recording sub-plots (Ministry of Forestry of Republic of Indonesia, 2013). The sample plots are regarding forest condition and representativeness of forest types.

Estimating the above ground biomass is applied in the area using a plot of regular shape of dimensions 20 x 20 m, 10 x 10 m, 5 x 5 m and 2 x 2 m, nested within each other, were defined as the unit for sampling (Figure 4-4). The details info that collected in the sampling plot (Appendix 5) is based on the Indonesia National Standard of Comprehensive and Regularly Forest Inventory rules.

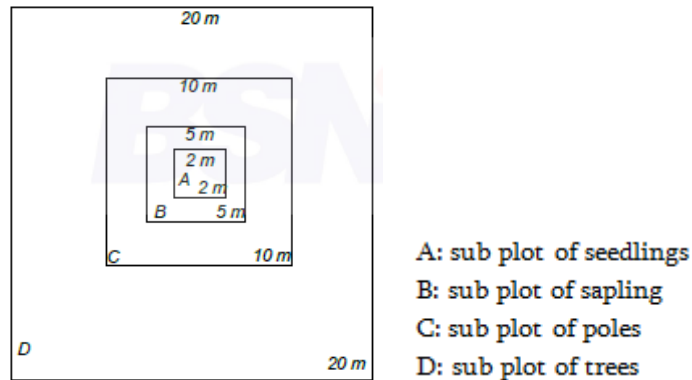


Figure 4-4. Dimension of the plot for biomass (Indonesia Nasional Standard of 7724, 2011)

4.2.3 Carbon estimation of airborne imagery

Segmentation of the imagery is done in eCognition software. Multi resolution segmentation is the most commonly used (Wardani, 2013). It creates image segments by considering scale, color, smoothness and compactness criteria. Multi resolution segmentation was selected since it can produces good shape of objects. For image objects, it minimizes the heterogeneity and maximizes homogeneity within the objects to produce meaningful objects. Segmentation is started by considering pixel as an object and then several objects are merged to homogenous bigger segments. Scale and shape parameters define this homogeneity. The object that finds best-fitting neighbor for merger merges in each loop until there is no possible to merge.

Determining the maximum scale parameter allows heterogeneity in the segmented objects. Choosing a high scale parameter produces larger object segments with a high amount of heterogeneity. Choosing a small-scale parameter generally produces more segments that are homogeneous. In this case, the optimum value based on the Estimation of Scale Parameter (ESP tool) for imagery photo of the research area is 21. ESP based on the local variance (LV) of heterogeneity at multiple scales of an image. The threshold point of changing LV indicates the

scale that the image can be segmented (Karna, 2012). Figure 4-5 shows the result of scale estimation using ESP tool.

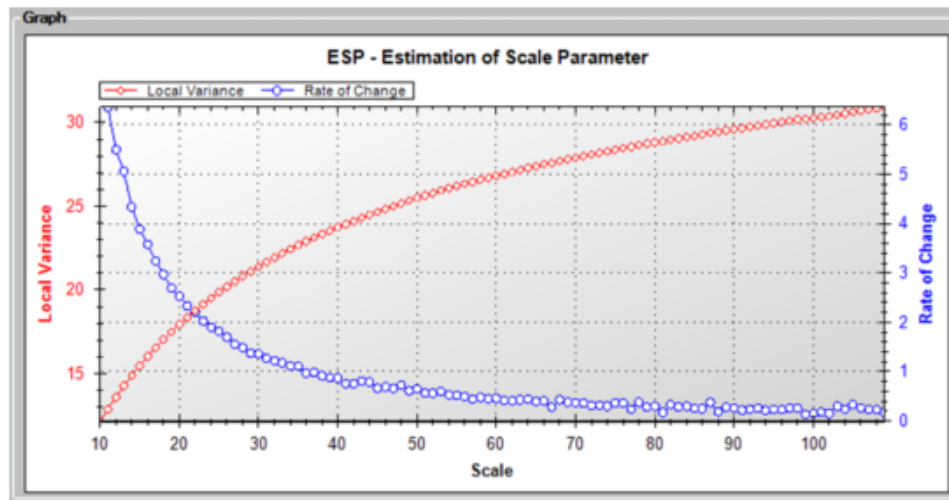


Figure 4-5. Scale estimation of ESP tool

Segmentation has algorithm that relies on pixel value and spatial continuity (texture and shape). The shape criterion indicates how much the spectral values of the image layers affect the heterogeneity of the segmented objects. Increasing the value of the shape field makes the image segments have more spatial uniformity and less spectral uniformity. The shape was set to 0.8 the example to produce more or less uniform shapes with little emphasis on the spectral uniformity. Meanwhile, the value 0.6 was used for compactness purposes to create high compact segments. The relation between scale parameter and composition of homogeneity is presented in Figure 4-6.

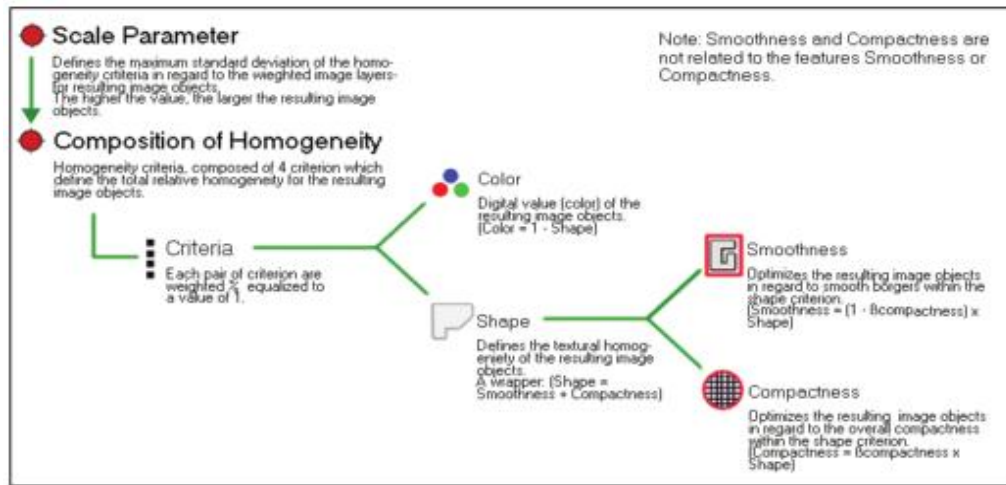


Figure 4-6. Concept of Multi resolution (Definiens, 2011)

The image was classified hierarchically by two levels (Figure 4-7). The first level purposes to distinguish shadow, vegetation, and non-vegetation. Separation of those levels was using brightness approach and some information such as mean and roundness.

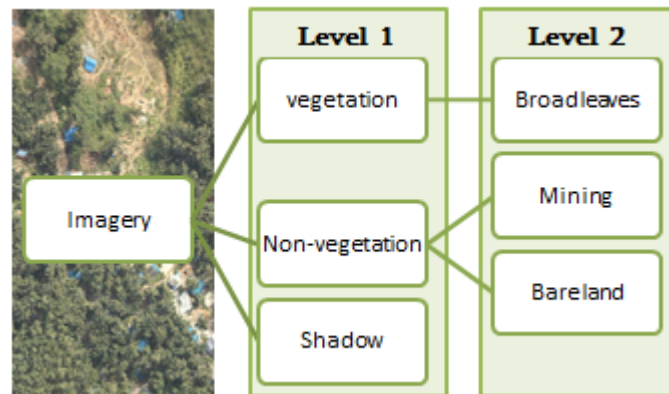


Figure 4-7. Hierarchy process in eCognition

To separate the segments, the watershed transformation algorithm was used. It considers the image as a topographic surface. It is made up of three basic notions: local maxima, catchment basins and watershed lines (Chen et al. 2004). An inverted distance map based on the inverted distances for each pixel to the image object border is calculated to determine the maximum distance from the edge. The

point which is farthest from the image object border is then taken as the local maxima. The distance from each point in the object to the local maxima are calculated. Based on the calculation all pixels within the specified threshold (distance) of the local maxima are put together as one new segment. This process is repeated, splitting image objects into smaller units, until splitting all image objects satisfy the threshold condition specified. Figure 4-8 shows rule sets of multi resolution segmentation in eCognition.

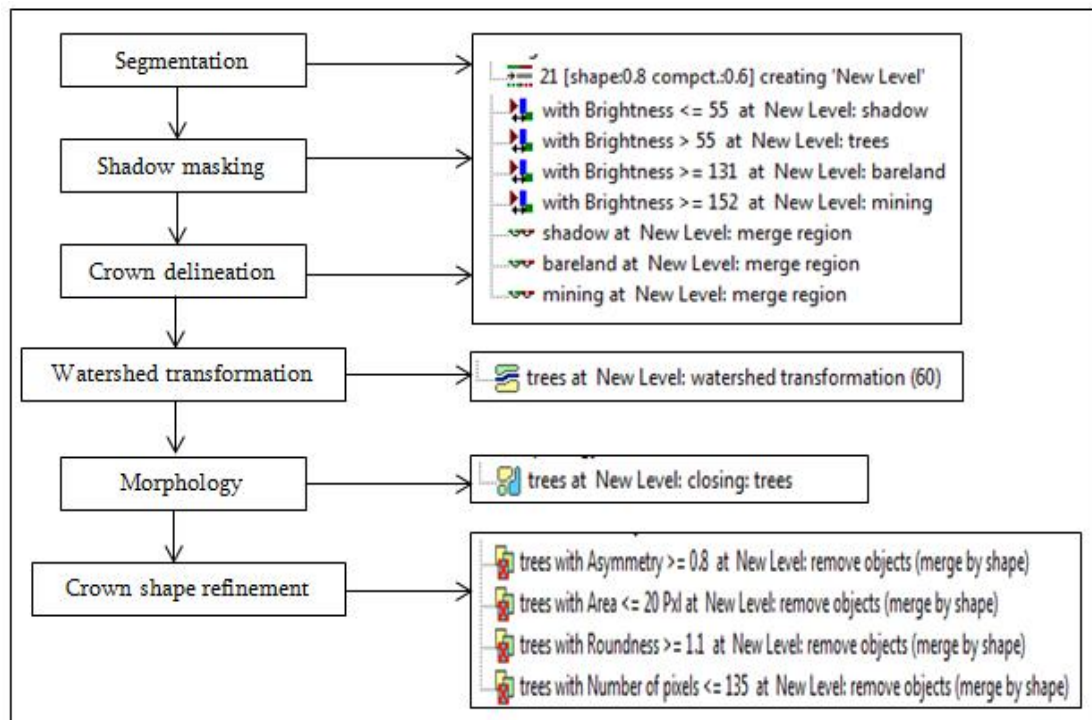


Figure 4-8. Rule sets of segmentation in eCognition

Fitting the crown segmentation with manual digitizing result drives to validate the result. At least 50 % of the object overlaps with the manual digitization; it was categorized as matching object. Those results were categorized into three types:

- Overlapped at least 50% (TP / True Positive)
- Less than 50% overlapped and not segmented automatically (FN / False Negative or omission error)

- c. Segmented but there was no existing tree (FP / False Positive or commission error)

Value of recall (r), precision (p), and accuracy (F) as studied by Li, et al. (2012) were used to calculate the accuracy of segmentation. Value of r, p and F are ranging from 0 to 1. Higher value means higher accuracy of segmentation.

$$r = \frac{TP}{TP+FN} \quad ; r \text{ represents object detection rate}$$

$$p = \frac{TP}{TP+FP} \quad ; p \text{ represents the correctness of the detection object}$$

$$F = 2 \times \frac{r \times p}{r + p} \quad ; F \text{ represents the overall accuracy taking both commission and omission errors into consideration}$$

Allometric equation which correlates DBH (Diameter at Breast Height) with total biomass can connect the carbon stock and segmented CPA (Crown Projection Area). Brown equation for tropical moist hardwoods (1997) was applied in the study area.

$$Y = \exp[-2.289 + 2.649 \cdot \ln(\text{DBH}) - 0.021 \cdot (\ln(\text{DBH}))^2]$$

where:

Y= aboveground dry matter, kg (tree)-1

DBH =diameter at breast height, cm

ln = natural logarithm

exp = “e raised to the power of”

Data of CPA and DBH from the image was modeled by validating using CPA and DBH in the field. The smallest error of regression model was chosen to estimate the above ground carbon (Wardani, 2013).

$$\text{Error} = 100 \times (\text{Carbon}_{\text{predict}} - \text{Carbon}_{\text{measured}}) / \text{Carbon}_{\text{measured}}$$

4.2.4 Post Fieldwork

The final step of this research is post-fieldwork, which is data analysis. Data collected from the study area and image analysis result provide the final maps. Map of gold mining pattern as well as forest cover map was processed using GIS software and image processing software. The last result was tree carbon map that describes the potential of carbon reserves of forest area where gold mining venture occupying.

5. RESULT AND DISCUSSION

5.1 Alteration of Landsat 8 OLI

5.1.1 Atmospheric correction

Figure 5-1 represents the original image and FLAASH-MNF corrected image of Landsat-8 OLI.

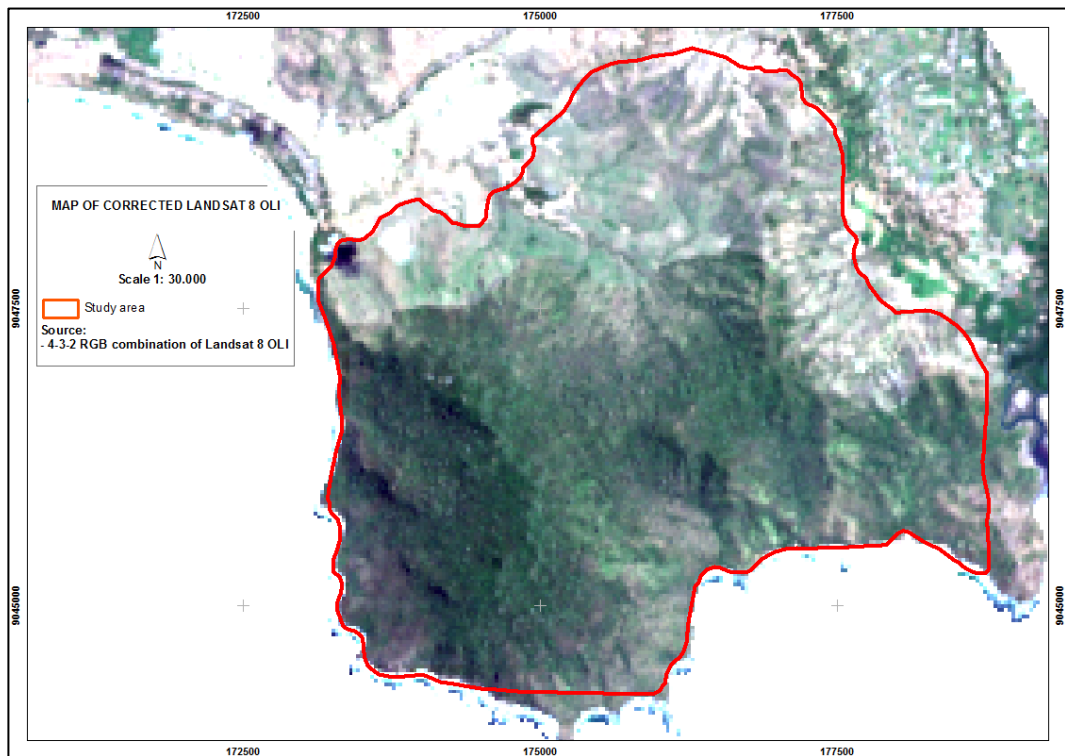


Figure 5-1. Atmospheric corrected of 4-3-2 composite band of Landsat-8 OLI

The final eigenvalues of Minimum noise fraction (MNF) is represented in Table 5-1. Eigenvalues for bands that contain information will be an order of magnitude larger than those that contain only noise. The bands (1, 2, 3, 4, 5, and 6) were useful from the MNF result. Band 7 showed the smallest value (eigenvalue less than 1 %) which indicates contain more noise than others do. It was caused by the presence of dense vegetation disturbs the absorption of 2.20 μm wave length that related to AlOH-MgOH content (Amin Beiranvand Pour, Hashim, & Marghany, 2014).

Table 5-1. The eigenvalue for the MNF bands result

MNF Band	Eigenvalue	Percentage (%)
1	131.61	69.47
2	24.79	13.08
3	11.73	6.19
4	8.66	4.57
5	6.30	3.33
6	4.59	2.42
7	1.76	0.93

5.1.2 Band ratio

Band ratio images increase the features contrast. Band ratio 4/2 is useful for mapping ferric iron oxides, due to it reflects highly in red region and absorbs in blue region (Ali & Pour, 2014). Band ratio 6/5 shows the ferrous iron oxide mineral mapping. Whilst, threshold statistic for the band ratio 6/7 (the ratio between shortwave infrared band) was 256.84 (Table 5-2). It posed no result for slice density of the clay mineral alteration in the area. This happens due to band 7 contains high noise based on the previous MNF result.

Table 5-2. Threshold of the Band ratio 4/2, 6/5, and 6/7

Band ratio	Mean	St-dev	Treshold	Max
4/2	155.38	39.31	194.69	255
6/5	204.54	24.99	229.54	255
6/7	254.98	1.86	256.84	255

By slicing the density of the band ratio, the each band ratio produced alteration of dominant mineral in the area. Band ratio of 4/2 and 6/5 highlight ferric iron oxides and ferrous iron oxides minerals in Landsat-8 OLI respectively (Figure 5-3 & Figure 5-4). Both minerals indicate the existence of iron / *Ferrum*).

High temperature type felsic rock melts is as driver or energy in iron oxide system (Australian Government Geoscience Australia). Therefore, gold is almost always

associated with iron or in other words the presence of iron oxide minerals plays role as one of indicators of Au features(“Natural Gold Indicators (Part 2) | RareGoldNuggets.com,” 2014).

Figure 5-2 reveals iron oxide such as limonite, jarosite and hematite tend to absorb from 0.4 to 1.1 μm (visible to middle infra-red) of the electromagnetic spectrum (Amin Beirandvand Pour & Hashim, 2014). Iron oxide highly reflects in the range of 0.63-0.69 μm , while vegetation reflects highly in 0.7-0.9 μm (NIR range). It causes iron oxide can be distinguish from vegetation.

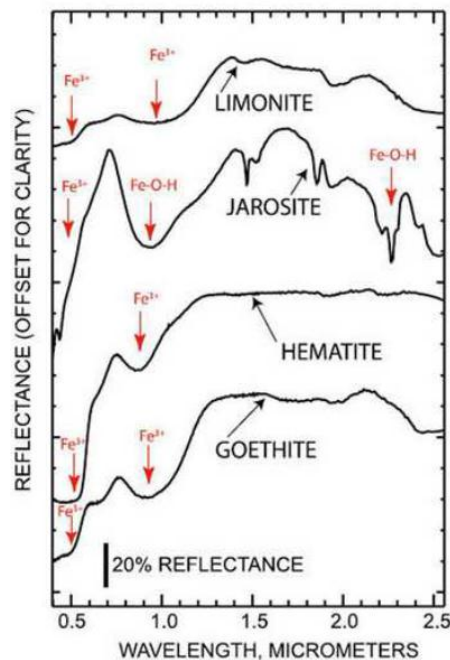


Figure 5-2. Spectral reflectance of Iron oxide minerals

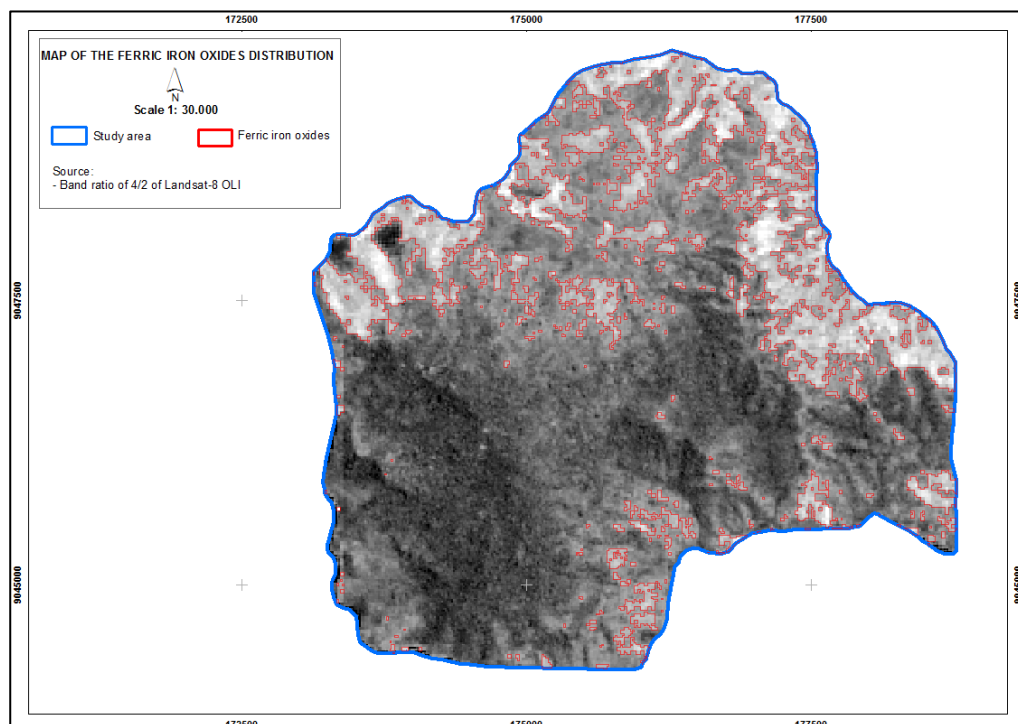


Figure 5-3. Ferric iron oxides distribution

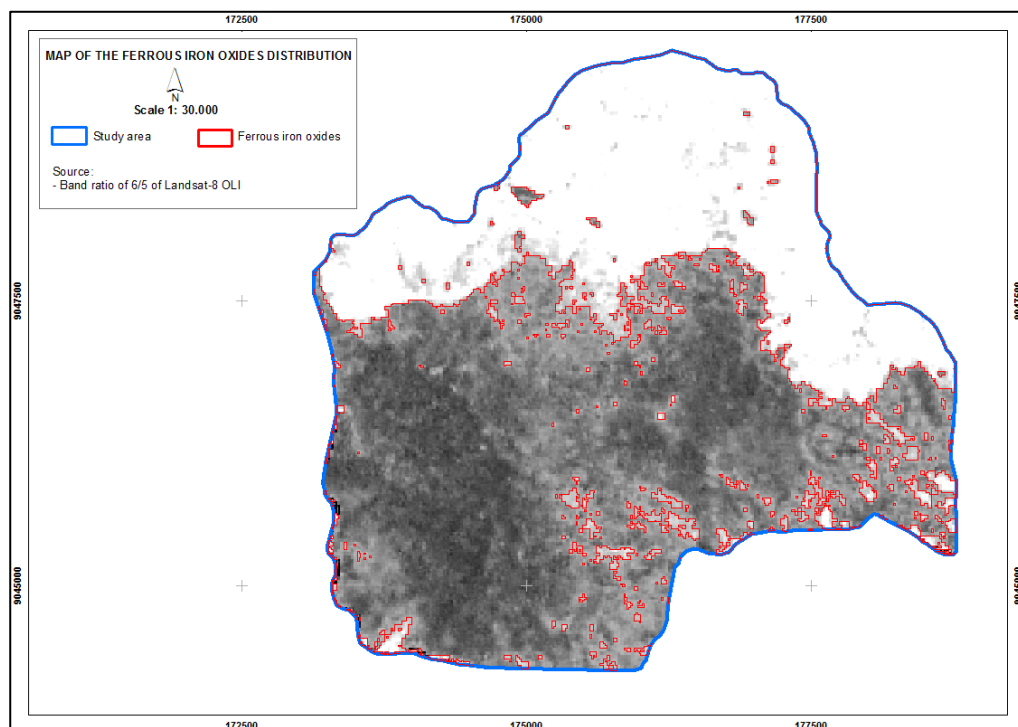


Figure 5-4. Ferrous iron oxide minerals distribution

5.1.3 PCA (Principal Component Analysis)

The result of PCA technique that applied in the area reveals the eigenvalue in PC1, PC2, PC3, and PC4 are 0.016, 0.006, 0.0033 and 0.00006 respectively. PCA shows the maximum variance of pixels (Kujjo, 2010). In this study, the first principal component consists of negative weighing of all total bands (Table 5-3). PC1 is about 63.33 % of eigenvalue of the total variance for data PCA. The eigenvectors loading of Band 2 and Band 4 in PC4 have negative and positive sign respectively, it can be predicted that iron-oxides will be distinguished by bright pixels in PC4. The eigenvector loadings (0.552282) for PC3 show that PC3 is dominated by vegetation (bright pixels), which highly reflects in Band 5. PC5 has opposite sign of Band 6 (negative) and Band 7 (positive), which maps Hydroxyl-bearing (clay) minerals as dark pixels.

Table 5-3. Eigenvalue and eigenvector of Principal Component Analysis result

PC image	Eigenvalue	Variance (%)					
PC1	0.015785	63.34					
PC2	0.005771	23.16					
PC3	0.003265	13.10					
PC4	0.000060	0.24					
PC5	0.000029	0.12					
PC6	0.000011	0.04					
PC7	0.000001	0.00					
Eigenvector	Band 1	Band 2	Band 3	Band 4	Band 5	Band 6	Band 7
Band 1	-0.044628	-0.058949	-0.123131	-0.188204	-0.529486	-0.676415	-0.453937
Band 2	0.342044	0.364828	0.354734	0.410930	-0.622671	0.090802	0.243399
Band 3	0.323834	0.333822	0.373336	0.251248	0.552282	-0.370584	-0.372613
Band 4	-0.211028	-0.172406	-0.121815	0.414958	0.141470	-0.586122	0.612504
Band 5	0.444107	0.377130	-0.194534	-0.624475	0.080171	-0.204124	0.429693
Band 6	-0.254372	-0.229329	0.816113	-0.410479	-0.021613	-0.108044	0.189811
Band 7	0.685330	-0.726255	0.029993	0.044021	-0.001087	-0.002562	0.005635

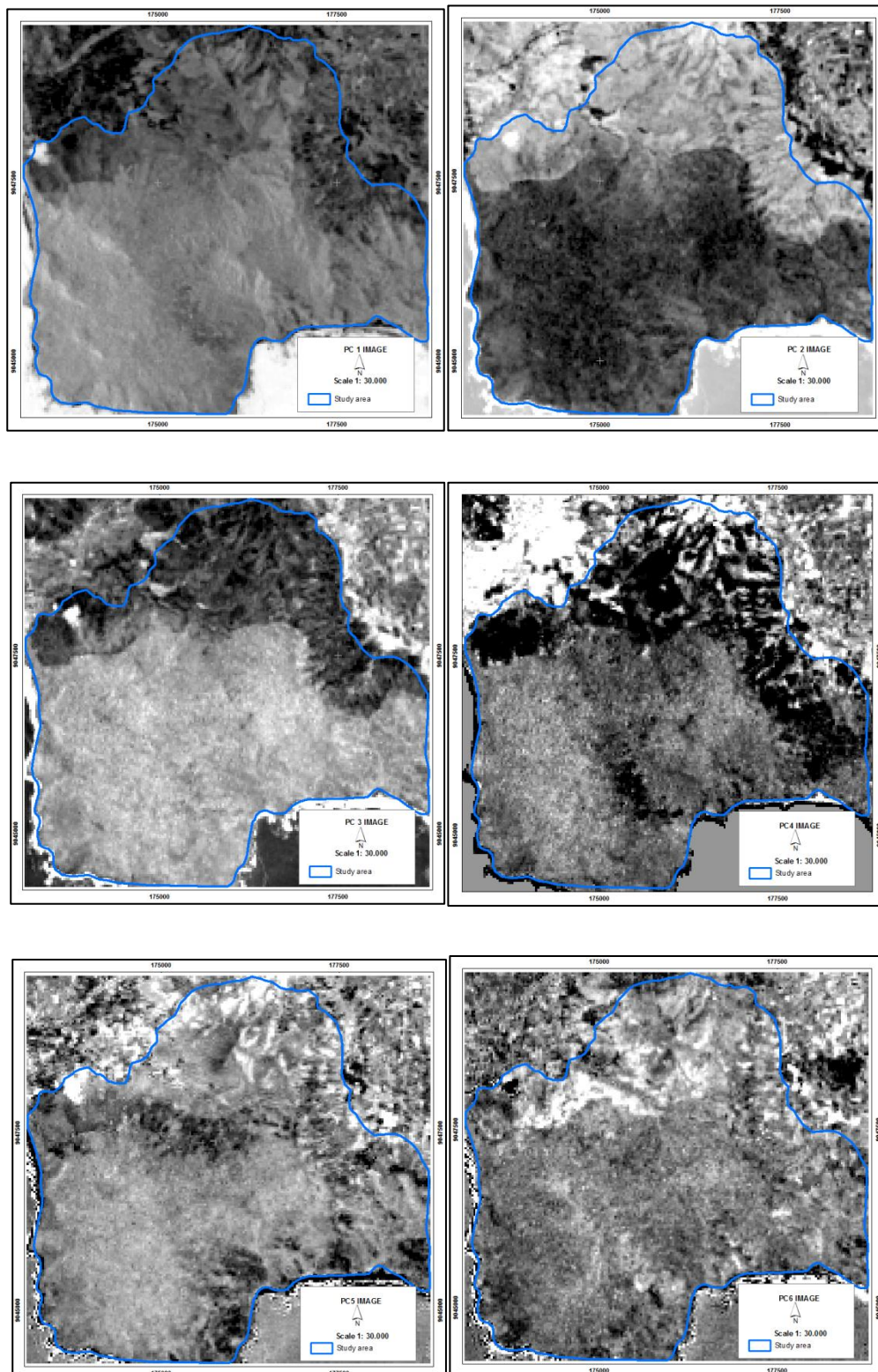


Figure 5-5. PC1-PC6 images of Principal Component Analysis

5.1.4 Lineament extraction

The hill shade model uses 315^0 viewing angle on the height of 45 km. This provides much linear edges where the dominant ridges are facing from North to South (Jordan & Schott, 2005). Figure 5-6 shows the result of automatic lineament extraction. The use of rose diagram can reveal major orientation of the lineaments (Abdullah et al., 2013). The dominant lineaments figure NW-SE of the major orientation. Automated results cover interval in N340W to N20E and S150E to S190W. The rose diagram of lineaments indicated that around 90 % of the lineaments fall in NW-SE. Table 5-4 reveals the basic statistic of number and length of the lineaments.

Table 5-4. Basic statistic of automated lineament result

Basic statistic	Value
Count	13
Minimum length (Km)	0.95
Maximum length (Km)	2.39
Sum (Km)	21.03
Mean (Km)	1.62
Standard Deviation	0.47

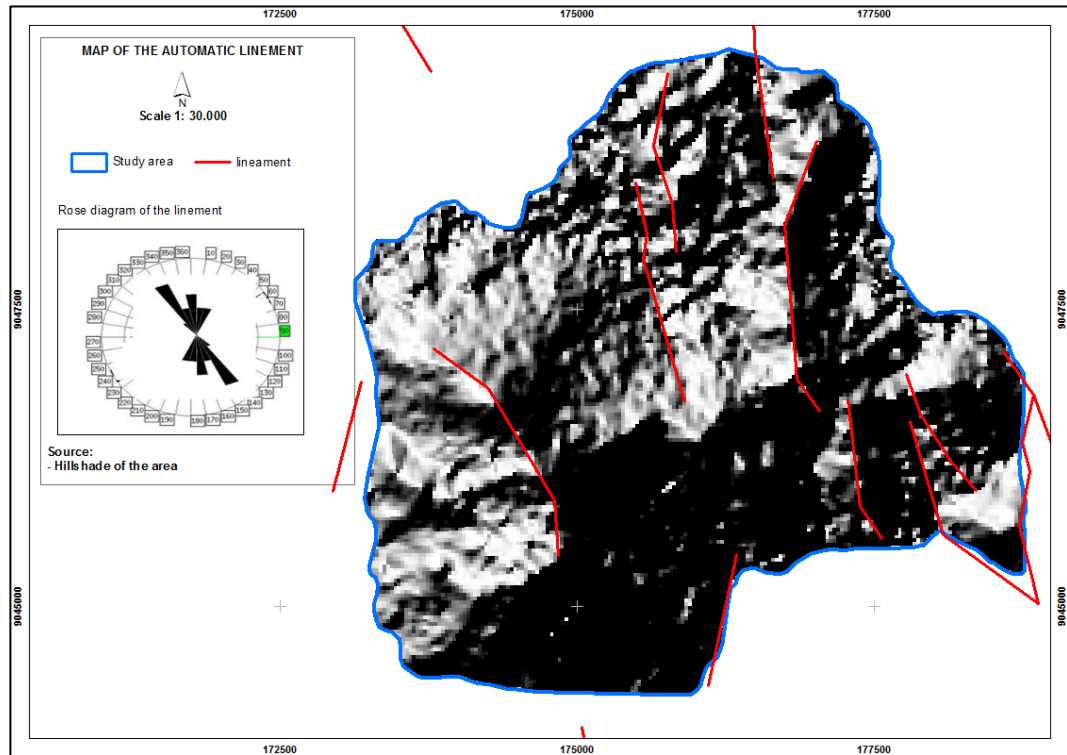


Figure 5-6. Automatic lineament in *PCI Geomatica* & rose diagram

Individual lineament often corresponds with structure such as faults (Caran, Jr, & Thompson, 1982). Figure 5-7 shows the fault based on the structural interpretation by Hellman & Schofield Pty Ltd (2009). Meanwhile, Figure 5-8 presents the existing fault and river distribution based on the Geology map. Automatic lineament mostly figured parallel to the 1st order faults. 1st order faults trend NW while 2nd order faults set trend ENE and WNW. The created automatic lineament is accompanied with major fault system. Therefore, the automatic result can be used to further analysis.

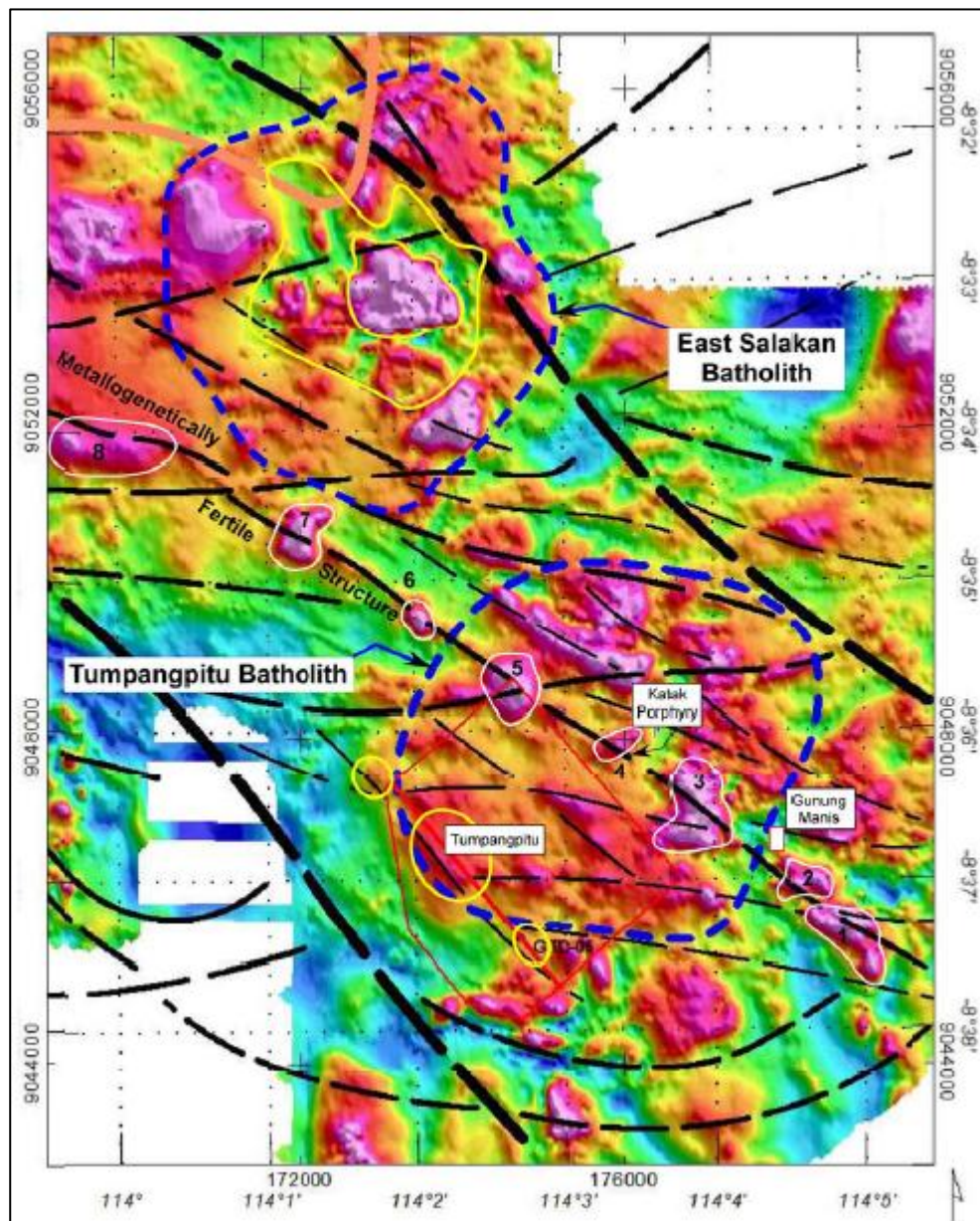


Figure 5-7. Regional fault system. 1st order is represented by thick dash lines

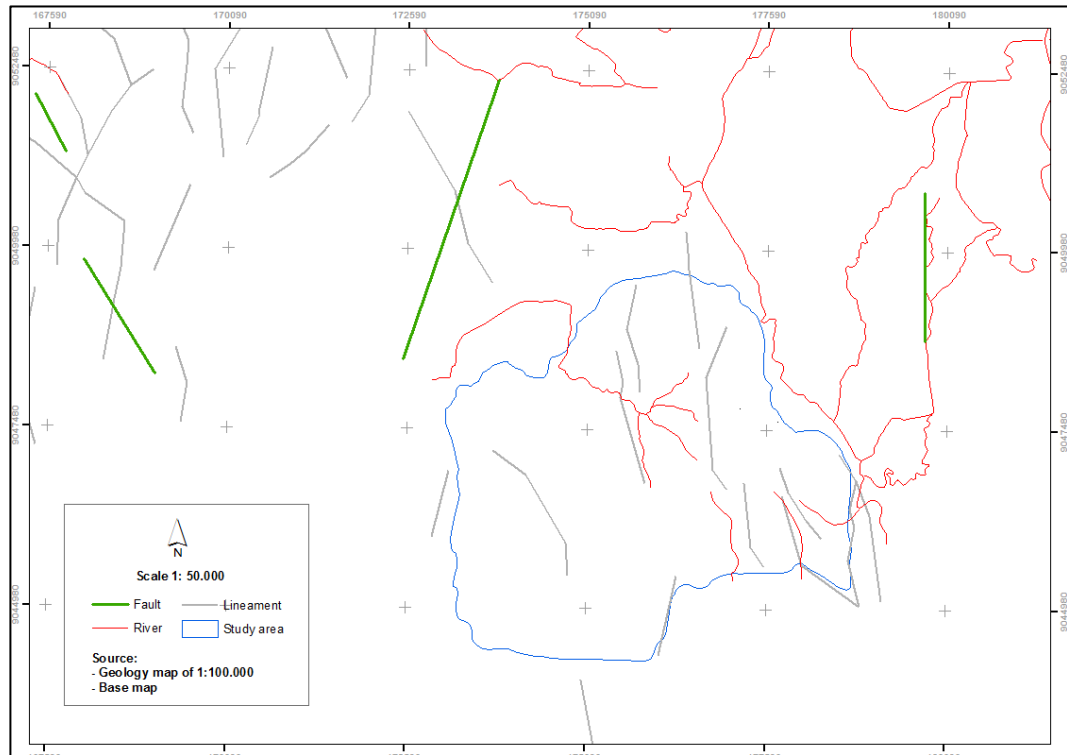


Figure 5-8. Fault system and river distribution based on the Geology map

5.1.5 Defining alteration zones

Shanks III (2012) stated that recognition of elements in altered rocks and identification of its zonal provides the metal deposits occurrence. Overlying previous result of band ratio 4/2, band ratio 6/5, extracted lineament and geology map resulted estimation of gold alteration zone in the study area (Figure 5-9). The association of ferric iron oxide, ferrous iron oxide mineral, automatic lineament result, as well as intrusive felsic type of rocks supports the gold reserves zone in the area.

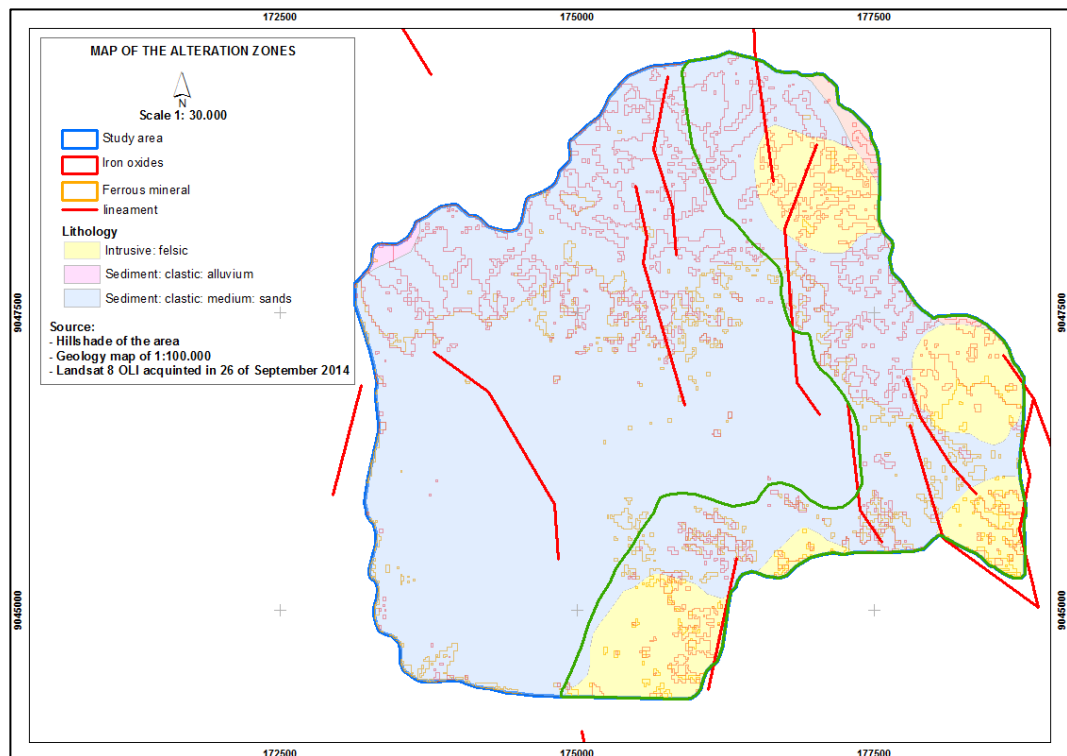


Figure 5-9. Estimated alteration zone

5.2 Current gold mining ventures

The existence of small-scale gold mining is in line with the previous analysis of Landsat image based gold alteration zones (Figure 5-10). Based on the category of small-scale mining in Indonesia, the operation in the study area is included in category III of illegal miners (Table 5-5).

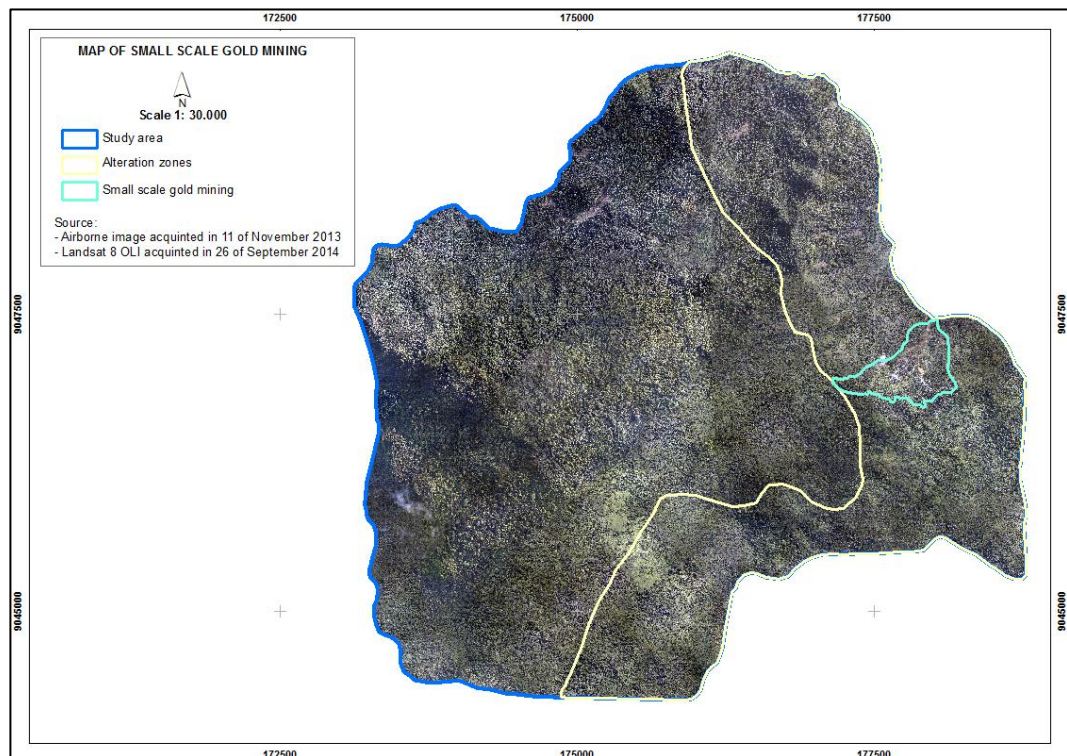


Figure 5-10. Small-scale mining location

Table 5-5. The Indonesia small scale gold mining category (Aspinall, 2001)

Small scale miners	Status	Financing	Regulatory Requirement	Estimated workers
Non-Regulated				
Nationals only	PETI- or illegal miners , mining gold and coal			
	1. PETI category I. Traditional Miners from mining location area. (casual workers)	Nil	Not Enforced	5,000
	2. PETI category II. Traditional Miners and those from out-side area (casual to full time)	Some	****	15,000
	3. PETI Category III. Traditional/Outsiders with out-side backers (full time)	A lot	****	60,000

Illegal miners - (or PETI- Pertambangan Tanpa Izin, or mining without permits) are identified by no permits. The operation sometimes held within mineral tenures of legal companies (Contracts of Work). This kind of operation without any care of the environment can cause big problem to the operators and government in the same time. According to Mining Colloquium (Energy and Mineral Resources Department, 2009), the number of miners in Tumpang Pitu area previously in

2008 reached three million people. They are indigenous from Kalimantan, Sulawesi, Nabire, and Bandung.

Previously, the miners did traditional dredging in the river (kucur). As a consequence, river became wider to 7 m from 1 m and deeper until 1.5 m from 0.5 m at the first (Energy and Mineral Resources Department, 2009). By the time external miner with higher capability of deep holes mining came to the area, many holes are formed. Based on the latest report of Perhutani (2014), the number of mining holes recently reached 368 active deep holes and 473 non-active holes. This type of mining operation draws much groundwater. Besides, the miners took the branches, twigs, and wood to build the tents. Most importantly, *ngasak* (locating the rocks surround the trees) damages the plantation. Mining activities were done by digging the ground to a certain depth and transporting the land that suspected containing the gold. Building on the measurement of soil layers at several deep ground sites, the thickness of soil is varied from one to five meters then followed by hard rocks beneath. The depth of mine holes varies between each team; which are ranging from 40-100 meters. This activity deprived the top layer fertile and created holes. The soil loss affected the thickness of soil layer. In addition, the holes could be filled by water and continuously reduce the soil. It increased the level of soil acidity that significantly influences the growth of plantation.

Recently, the number of illegal miner in study area was estimated to 4400 people, of whom 4382 people were actively mining in plot 78 and 34 people in plot 79 (Perhutani, 2014). From observation and conversation with the miners, a mining team for deep ground mining, typically consisted of five to ten workers. On the other hand, mining activity along the river individually operated.

Related to the position of deep ground mining by the illegal miners, they just can get the gold from the vein due to the limitation of resources. Based on the observation and interview, the team member manually digs the rocks and follows the vein track. In addition, another limitation of illegal miners is related to the processing ability / amalgamation of the ore. The miners directly use mercury to amalgam the gold. Those characteristics above is in accordance with the

characteristic of small-scale gold mining types in Indonesia studied by Aspinall (2001). Inadequate usage of mercury in processing stage to obtain gold metal became another issue. Susintowati (2012) stated that mercury contamination in sediment reached 0.45 ppm and reached 1.17 ppm at the creek. It exceeds the normal limit of 0.1 ppm for mercury level in the nature (Decree of Ministry of Environment, 2004).

5.2.1 Forest cover condition

Inadequate mining operations damage vegetation cover and forest function (Musa & Jiya, 2011). Imageries are useful to provide information about percentage of vegetation cover. The major damage to the plantation was building the tent in vegetated area and the using of wood as mining equipment.

Table 5-6. Percentage of forest cover

No	Forest cover		Area (Ha)	Percentage (%)
	Cover	Crown Density (C)		
1.	Bare land	-	0.46	1.24
2.	Mining	-	14.49	39.10
3.	Production forest	C1	3.33	8.99
		C2	5.16	13.92
		C3	2.02	5.45
		C4	11.6	31.30
Total			37.05	100.00

By 2013, the area that directly affected by small-scale gold mining ventures reached 14.49 ha or had occupied for about 39.10 per cent of total area (Table 5-6). This region can be widespread think of the alternation zone that reaches to 796.55 ha and low control of the management. Miner occupied area along the river and deep ground holes that are remarkable by the colorful tents (Figure 5-11). Meanwhile, area of production forest that affected was around 59.66 per cent. It is similar to a study by Tom-Dery, Dagben, & Cobbina (2012) in Northern Ghana who found that mining significantly affected vegetation cover.

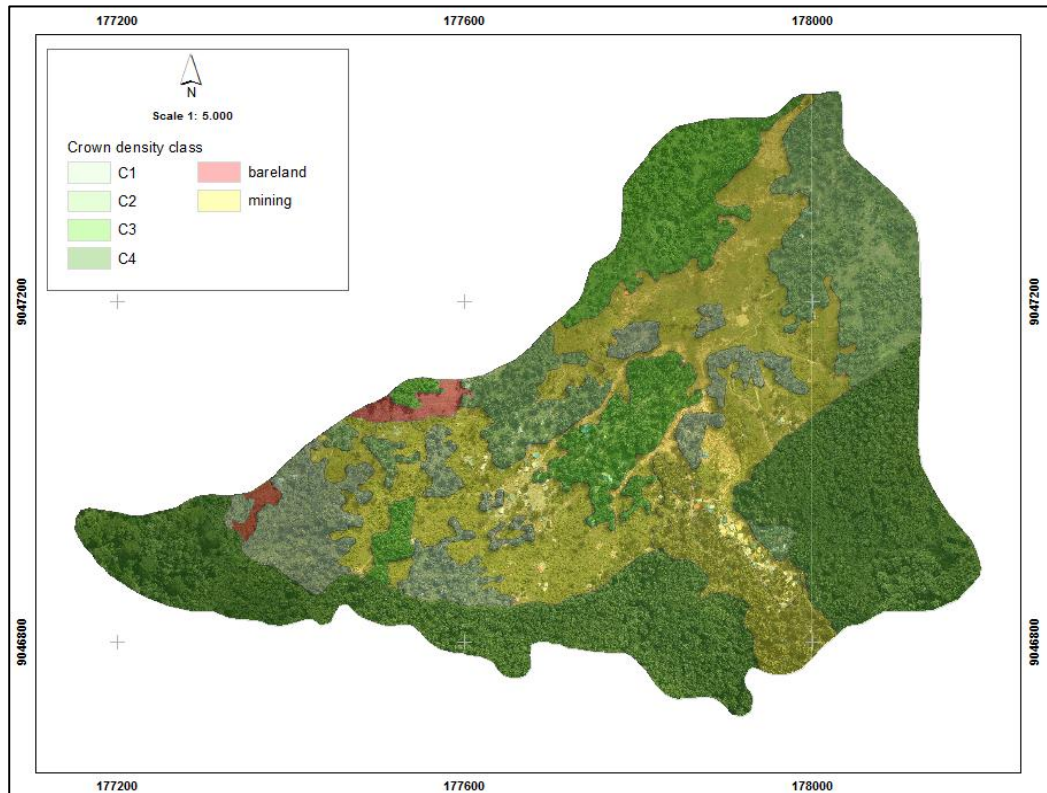


Figure 5-11. Mining distribution

Manual delineation of mining location had limitation due to the distribution of mines. The deep ground mine that located between the dense trees sometimes could not be recognized on the airborne imagery.

5.3 Carbon estimation

5.3.1 Descriptive of trees attributes

The descriptive statistics of DBH and CPA is presented in Table 5-7. The DBH has a mean and a standard deviation of 23.4 cm and 2.6 cm respectively. Similarly, the CPA has a mean and a standard deviation of 38.2 m² and 10.2 m² respectively.

Table 5-7. Descriptive statistic of trees

Attributes	Minimum	Maximum	Mean	Std.Deviation
DBH	19.4	29.9	23.4	2.6
CPA	18.8	70.8	38.2	10.2

5.3.2 Result of segmentation

Figure 5-12 shows example of the result of segmentation process of the 2013 airborne imagery.

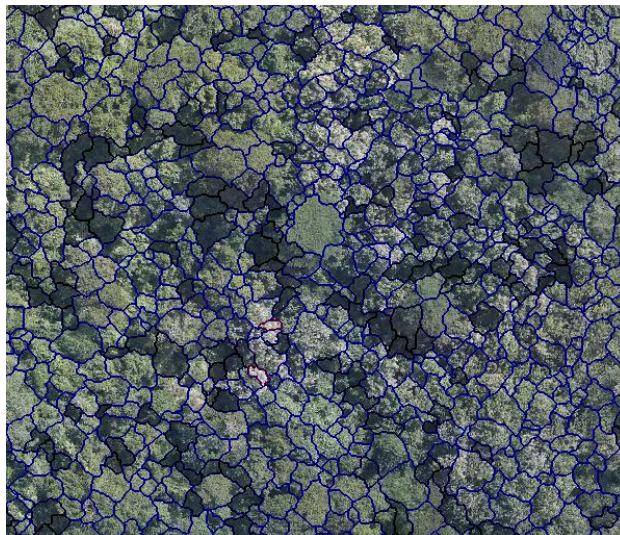


Figure 5-12. Example of the airborne imagery segmentation

The result of digital segmentation in eCognition indicated several errors. Shadowed areas were mostly found on the western aspect where located at the reverse of the hill. These areas take less sunlight at daytime and it was shadowed at the time of image capture.

5.3.3 Segmentation accuracy

Manual digitization was done to determinate whether segmentation was overestimate or underestimated. Validation method by Li et al. (2012) was applied to calculate the accuracy. Table 5-8 reveals the value of r, p and F of segmentation

result. The percentage of TP / overlapped segmentation shows 67 % which means over segmentation error. Yet, high value of r, p and F (>50 %) means good accuracy of segmentation result and acceptable to be used in analyzing the carbon estimation.

Table 5-8. The validation of segmentation

Tree	Number of Tree	TP		FN		FP		r	p	F
		N	(%)	n	(%)	n	(%)			
Broadleaves	11656	7809	67	2762	24	1084	9	0.74	0.88	0.80

5.3.4 DBH-CPA-Carbon relationship

Model of Crown Projection Area (CPA)-Carbon of trees based on Linear, Logarithmic, Quadratic, and Power regression can be shown in Table 5-9.

Table 5-9. Model of DBH-CPA and CPA-Carbon of trees

DBH-CPA Model		R ²	Error (%)
Linear	$DBH = 15.21 + 0.21 CPA$	0.54	15.3
Logarithmic	$DBH = 17.16 \ln CPA - 3.66$	0.49	10.9
Quadratic	$DBH = 0.002 CPA^2 - 0.05 CPA + 18.2$	0.54	14.5
Power	$DBH = 16.6(1.009^{CPA})$	0.53	11.1
CPA-Carbon Model		R ²	Error (%)
Linear	$Carbon = 20.94 + 4.06 CPA$	0.54	8.3
Logarithmic	$Carbon = 141.81 \ln CPA - 337.36$	0.50	7.3
Quadratic	$Carbon = 0.05 CPA^2 - 0.06 CPA + 97.2$	0.55	10.7
Power	$Carbon = 71.7(1.03^{CPA})$	0.53	7

The power model of DBH-CPA relationship has the best criteria among others. The power model was also used to estimate the carbon from CPA variable. Higher value of R² shows that higher chance of the independent variable can define dependent variable. Whilst, smaller value of error means that input variable generates small error to determine the output. The description of accuracy

assessment of DBH-CPA and CPA-Carbon relationship is presented in Appendix 6 and 7.

5.3.5 Tree carbon estimation

5.3.5.1 Total tree carbon

Based on the Schnitzler (2010) the dry biomass of tropical rainforests range from 150-850 ton organic dry substance per hectare. In addition, Condit (2008) resumed some inventories about aboveground biomass in tropical rainforest. The amount of aboveground biomass in tropical forest of Panama, Malaya, and Borneo was 260, 303.6 and 433.7 ton/ha respectively. Furthermore, Brown (1997) stated that trees play as primary element in estimating above ground biomass and unit carbon equals to half of its biomass (Brown, et al., 1993)

Defining subsets to estimate carbon of trees on the alteration zone and non-alteration zone could give clear comparison. From the result, it can be known that the sample plot in alteration zone resulted 176.97 tons/ha of carbon. Meanwhile, the carbon of non-alteration zone reached 235.82 tons/ha. In total, the amount of carbon in study area was 386519.14 tons.

Based on the result of tree crown segmentation, the amount of carbon stored of broadleaves trees in the study area is represented by Table 5-10.

Table 5-10. Total carbon of the study area

Study area	Value	Zone	Carbon (Ton/ha)
Total extent (ha)	2101.89	Alteration	176.97
Total carbon (ton)	386519.14	Non-alteration	235.82
Average carbon (ton/ha)	183.89		

5.3.5.2 Tree carbon of small scale gold mining area

Defining the tree carbon focused on the small-scale mining area is purposed to know the direct influence of mining to carbon reserves. Total tree carbon in small

scale gold mining area estimated to 4808 tons with average of 129.78 ton/ha (Figure 5-13). Based on the types of rock beneath, the average carbon of intrusive felsic types rocks reached 127.27 ton/ha and 131.68 tons/ha of sediment clastic types (Table 5-11). Sreejesh et.al, (2013) stated that the mean biomass of 15 year Teak plantation in Kerala was 223.14 ton/ha or around 111.57 kg/tree. Meanwhile, Chanan (2012) studied estimation of above ground carbon in Perhutani of Malang East Java and found that carbon stored was about 109.4 ton/ha of second age class of Teak.

Table 5-11. Carbon of the subset area

Small-scale mining	Value	Lithology	Carbon (Tons/ha)
Total extent (ha)	37.05	Intrusive felsic	127.27
Total carbon (tons)	4808.28	Sediment clastic	131.68
Average carbon (tons/ha)	129.78		

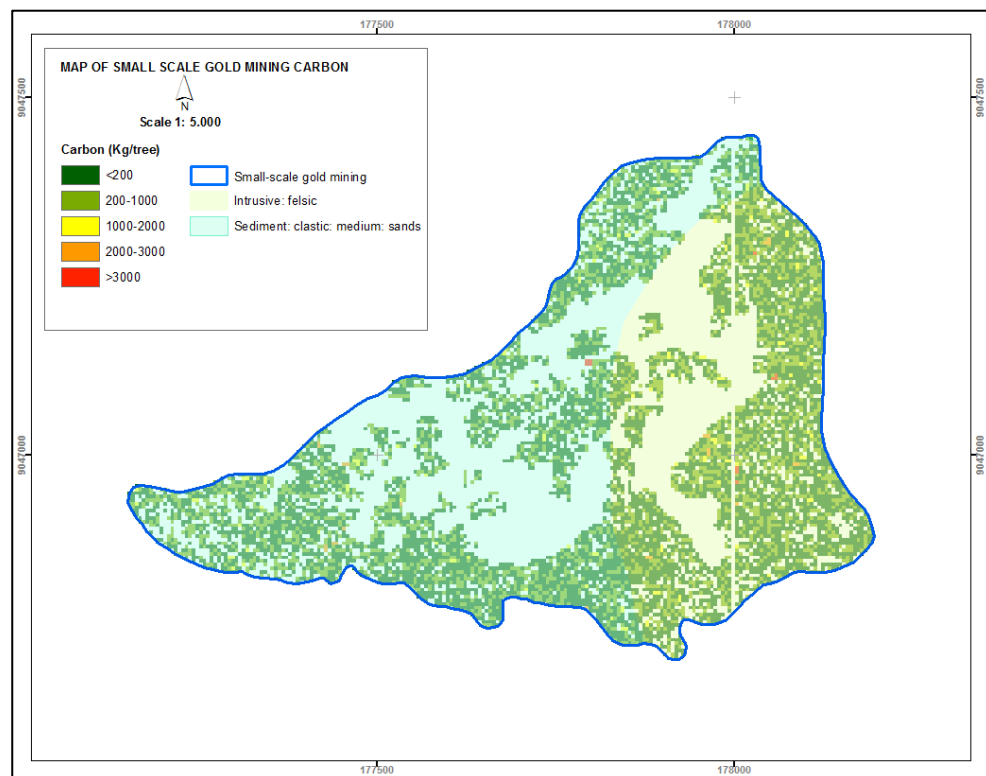


Figure 5-13. Distribution of the tree carbon

5.3.6 Analysis of the factor

Environment factors influencing plant growth are complex (Billings, 1952). However, study of the effect of such single factor is necessary since change in one factor affects the others. Parent material factor has some aspects such as mineral presents, structure and weathering susceptibility. In addition, the rate of species growth depends on the mineral composition of soil and parent rock (Raina & Gupta, 2009). Tree growth depends to the extent of the minerals as soil nutrients derived from weathering process.

Role of parent material in plant growth can be assessed using indicators namely height, DBH and crown area. In terms of airborne imagery application, the parameters that can be obtained are DBH and crown area. The estimated tree carbon model was applied to the whole study area with some assumptions; broadleaves species type and similar lithology formation types dominated by sediment clastic and intrusive felsic. Table 5-12 presents the comparison that studied in carbon estimation.

Table 5-12. Comparison of area of carbon class

Factor	Sub-factors	Area of carbon class (ha)				
		<200	200-1000	1000-2000	2000-3000	>3000
Alteration zone	Alteration zone	348.93	190.66	8.03	1.69	1.48
	Non-alteration zone	481.59	240.88	8.95	1.73	1.46
Slope	0-2% (flat)	21.52	9.92	0.46	0.05	0.08
	2-7% (gently sloping)	67.89	34.39	1.44	0.35	0.35
	7-15% (sloping)	138.74	65.97	2.44	0.49	0.39
	15-30% (moderately steep)	376.00	192.46	7.18	1.49	1.16
	30-70% (steep)	219.58	124.52	5.28	1.02	0.91
	70-140% (very steep)	0.49	0.38	0.02	0.00	0.01
Parent rock	Extrusive intermediate lava	6.46	3.34	0.17	0.03	0.03
	Sediment clastic: medium sands	678.12	352.05	13.92	2.81	2.41
	Sediment clastic: alluvium	3.02	1.30	0.04	0.01	0.02
	Intrusive felsic	142.63	74.64	2.83	0.57	0.48

Analysis factor of multivariate statistic was applied to define factor that dominantly affects carbon quantity. The communalities result showed that all of

the factors above could describe the carbon content (Appendix 8). However, the sub-factor alteration zone, 2-7% of slope, 15-30% of slope, sediment clastic, and intrusive felsic had high influence to the carbon amount (value of extraction ≈ 1).

Influence of slope factor is correspondingly with the study of Raina & Gupta (2009) who stated that the structure of plant communities seems to be primarily influenced by altitudinal variation. Wysocki, et al. (2011) stated that slope gradient plays role as energy measurement that drives mass movements. In addition, soil surveyors use slope variations as indicators of soil changes in landscapes. In conclusion, changing in slope possibly changes the plant growth due to different soil as plant nutrients.

As mountains, Tumpang Pitu represents unique geomorphic related to slope complexity. Wysocki, et al., (2011) mentioned that in humid climate, mountaintops, characterized by simple slopes of short transport colluvial sediments, have quite thick soil. The mountainside (*mountainflank*) characterized by complex slopes and long transport colluvium. Meanwhile, mountain base has thick colluvium. These characteristics can describe the quantity of tree carbon stock of moderately steep, step, and sloping slope in the study area became higher than the rest slopes. In contrary, low slope gradients results minimal erosion by running water. As consequences, fluvial drainage poorly developed.

The effect of the altered mineral on plant growth relates to the presence of hydrogen-ion concentration (Billings, 1950). Based on the experiment, Billings found that the growth of tomato and tobacco in altered andesite had much lower height grow than unaltered one. The chemical characteristic of altered andesitic soil also showed higher acid insoluble (mostly SiO_2) and lower pH (acid type). Lacking of essential elements of phosphorus and available nitrogen becomes matter to plant growth in altered area. However, in altered area of this research is used to grow the Teak plantation. The selection of Teak species had been adjusted with the ability of Teak species to grow (Appendix 9). It posed the plantation still can grow in the area even tough in low growth.

In terms of parent rock, intrusive rock comes from magma that intruded and cooled below the earth surface. The felsic classification means the rock contains a lot of feldspar or silica, sodium, calcium and quartz ("Igneous Rocks," n.d.). The common type of intrusive rock is granite which is formed over long period and very hard. Intrusion of diorite is also mapped in study area (Hellman & Schofield Pty Ltd, 2011). This kind of altered rocks requires root to penetrate deeply (Billings, 1952). Meanwhile, sedimentary rock comes from sediments of weathered rock by the wind, running water or the sea. The dominant types in the study area are sediment clastic: medium sands. Sediment clastic (Singh & Huat, 2012) forms from fragments of pre-existing rocks (clast) and usually contains layering. Especially in cool-humid vegetated area, the accumulation of dead leaves and plants debris decomposed and produced weak acids that accelerate the weathering (Raj, 2005). The top layer consists of clays (kaolinite, carbonates and reduced iron materials), followed by sandy soils with underlain clays, weathered parent materials and then parent rock. These differences of intrusive and sediment might pose the growth of vegetation above both parent rocks.

6. CONCLUSION AND RECOMMENDATION

6.1 Conclusion

Gold mining ventures affected forest condition. The following conclusions are based on the specific objectives as formulated in the introduction chapter.

1. To identify the gold alteration zones distribution using imageries

1.1 What are the proper techniques required to generate alteration zones

Gold alteration zone from Landsat-8 OLI requires atmospheric correction of FLAASH and MNF first followed by band ratio. Band ratios of 4/2 and 6/5 highlighted ferric iron oxides and ferrous iron oxides minerals in the area of interpretation. Meanwhile, band ratio 6/7 that applied was not resulted clay mineral potential. Principal Component Analysis applied in Landsat-8 OLI illustrated the iron-oxides and hydroxyl altered minerals. LINE algorithm in PCI Geomatica software extracted lineament by processing the hill shade image of DEM. All of those parameters added with the information of rock types could estimate the alteration zone.

2. To estimate the trees carbon of the gold alteration zones

2.1 How much the difference of carbon content between alteration and non-alteration zones

From the calculation, it can be seen that alteration zone had smaller carbon content than non-alteration zone. The difference was reached about 58.85 ton/ha.

3. To identify and detect a small-scale gold mining setup using high resolution airborne multispectral imagery

3.1 How accurately can a gold mining and its spatial pattern be detected in the study area

The small-scale gold mining can be detected manually by interpreting 2013 airborne imagery. It resulted 14.49 ha of illegal mining. On the other hand, based on the report of Perhutani in March 2014, the extent of small-scale mining focused in plot of 78 and 79 was 7 ha. The difference

was resulted due to the different time of acquired data of airborne imagery and field check by the management of Perhutani. Moreover, there was cover up of the non-active mining holes and policing enforcement by the authorities.

3.2 What is the condition of vegetation cover and its pattern in an area of gold mining?

Vegetation cover is disturbed by the existence of mining activities especially deep holes type of mining. The miners build tents between the trees causes root weak which can make the tree to get fall if exposed to strong wind. The pattern of vegetation cover influenced by gold mining is revealed by Figure 5-10.

3.3 How accurately can carbon stock lost to degradation because of gold mining be estimated and mapped using high-resolution airborne multispectral imagery and OBIA?

Segmentation using OBIA in MS airborne imagery resulted with reasonable overall accuracy which was 0.8. It means that the model generated from crown segmentation can be applied in carbon estimation. In terms of the carbon model used, the power model has R^2 and RMSE that can be accepted to estimate the carbon.

3.4 How much carbon stock have lost for forest degradation because of mining activities in small scale gold mining area?

Carbon estimation of small-scale mine area had differences of 47.19 ton/ha fewer compare to the area in the same alteration zone and 106.64 ton/ha less than non-alteration zone. It proves that mining activity affected the carbon reserves that can be stored in a forest area.

4. To recognize the factors that influence carbon distribution

4.1 What are the factors that influence the carbon distribution?

Based on the result of analysis factor, alteration zone, slope of area and parent material influence carbon reserves. The alteration zone carbon result showed fewer amounts than non-alteration zone. Slope of the area also affects carbon distribution. Moderately steep slope (15-30 %) gave

higher impact of carbon reserves which is contrary to the gently slope (2-7 %). In terms of rocks, sediment clastic became sub-factor that high influence carbon reserves.

6.2 Recommendation

Aerial photography offers improved vantages over ground based observation. It provides better spatial resolution and geometric/ radiometric fidelity especially for small area interpretation. For further identification of vast gold mining region, it can be integrated between satellite imagery that has good spectral range and LiDAR to determine the height of tree in term of carbon estimation.

Related to the this study limitation of soil properties, it is recommended for further analysis to collect field soil samples in order to obtain specific and actual parameters of soil.

LIST OF REFERENCES

- Abdullah, A., Nassr, S., & Ghaleeb, A. (2013). Landsat ETM-7 for lineament mapping using automatic extraction technique in the SW part of Taiz area, Yemen, *13*(3).
- Ali, A., & Pour, A. (2014). Lithological mapping and hydrothermal alteration using Landsat 8 data: a case study in ariab mining district, red sea hills, Sudan. *International Journal of Basic and Applied Sciences*, *3*(3), 199–208. <http://doi.org/10.14419/ijbas.v3i3.2821>
- Alvarez-Berríos, N. L., & Mitchell Aide, T. (2015). Global demand for gold is another threat for tropical forests. *Environmental Research Letters*, *10*(1), 14006. <http://doi.org/10.1088/1748-9326/10/1/014006>
- Aspinall, C. (2001). Small-scale mining in Indonesia, (79).
- Australian Government Geoscience Australia. (n.d.). 2.4 Iron oxide copper-gold mineral systemtAustralia. Retrieved from <http://www.ga.gov.au/data-pubs/data-and-publications-search/publications/critical-commodities-for-a-high-tech-world/iron-oxide-copper-gold>
- Berk, a., Bernstein, L. S., Anderson, G. P., Acharya, P. K., Robertson, D. C., Chetwynd, J. H., & Adler-Golden, S. M. (1998). MODTRAN cloud and multiple scattering upgrades with application to AVIRIS. *Remote Sensing of Environment*, *65*(3), 367–375. [http://doi.org/10.1016/S0034-4257\(98\)00045-5](http://doi.org/10.1016/S0034-4257(98)00045-5)
- Billings, W. D. (1950). Vegetation and plant growth as affected by chemically altered rocks in the Western Great Basin. *Ecology*. Retrieved from http://www.jstor.org/stable/1931361?seq=7#page_scan_tab_contents
- Billings, W. D. (1952). The environmental complex in relation to plant growth and distribution. *The Quarterly Review of Biology*. <http://doi.org/10.1086/399022>
- Blaschke, T., Lang, S., Lorup, E., Strobl, J., & Zeil, P. (2002). Object-oriented image processing in an integrated GIS / remote sensing environment and perspectives for environmental applications, 555–570.
- Bodruddoza Mia, M., & Fujimitsu, Y. (2012). Mapping hydrothermal altered mineral deposits using Landsat 7 ETM+ image in and around Kuju volcano, Kyushu, Japan. *Journal of Earth System Science*, *121*(4), 1049–1057. <http://doi.org/10.1007/s12040-012-0211-9>

- Brown, S. (1997). Estimating Biomass and Biomass Change of Tropical Forests: a Primer. (FAO Forestry Paper). Retrieved April 10, 2015, from <http://www.fao.org/docrep/w4095e/w4095e00.HTM>
- Brown, S., Iverson, L. R., Prasad, A., & Liu, D. (1993). Geographical distributions of carbon in biomass and soils of tropical Asian forests. *Geocarto International*, 8(4), 45–59. <http://doi.org/10.1080/10106049309354429>
- Caran, S. C., Jr, C. M. W., & Thompson, E. J. (1982). Lineament analysis and inference of geologic structure : examples from the Balcones Ouachita trend of Texas, XXXI.
- Center of Soil Research. (1982). Indonesia soil classification (in Indonesia).
- Chanan, M. (2012). Estimation of above ground carbon on Teak plantation (*Tectona grandis* Linn.F)(in RPH Sengguruh BKPH Sengguruh KPH Malang Perhutani East Java) (in Indonesia), 7(C), 61–73.
- Charou, E., Stefouli, M., Dimitrakopoulos, D., Vasiliou, E., & Mavrantza, O. D. (2010). Using remote sensing to assess impact of mining activities on land and water resources. *Mine Water and the Environment*, 29(1), 45–52. <http://doi.org/10.1007/s10230-010-0098-0>
- Chevrel, S., Bourguignon, A., Cottard, F., & Itard, Y. (2005). Exploitation of ASTER imagery in mining-related environmental management.
- Chupezi, T., Ingram, V., & Schure, J. (2009). Impacts of artisanal gold and diamond mining on livelihoods and the environment in the Sangha Tri-National Park landscape. Retrieved from http://www.cifor.org/publications/pdf_files/books/bchupezi0901.pdf
- Colaborative Partnership on Forest (CPF). (2014). Assessment and monitoring of forest degradation. Retrieved August 11, 2014, from <http://www.cpfweb.org/73032/en/>
- Communication and Information Agency. (2009). Environmental agency monitor the Banyuwangi mining exploration. Retrieved April 20, 2015, from <http://kominfo.jatimprov.go.id/watch/18195>
- Condit, R. (2008). Methods for estimating aboveground biomass of forest and replacement vegetation in the tropics. *Center for Tropical Forest Science Research Manual*, (August), 73 pages.

- Decree of Minister of Environmental. (2004). Decree of Minister of Environmental of 51 of sea water standard (in Indonesia).
- Definiens. (2011). *eCognition Developer 8.7 reference book*. Munchen Germany.
- Energy and Mineral Resources Agency. (2013). Strategic minerals in Districts (in Indonesia). Retrieved from <http://webmap.psdg.bgl.esdm.go.id/geosain/neraca-mineral-strategis.php?mode=administrasi>
- Energy and Mineral Resources Departement. (2009). 2009 Mining colloquium (in Indonesia) (pp. 978–979).
- Erk, A. Van. (2011). Application of remote sensing for ecosystem services monitoring in tropical forest conservation, (September).
- FAO. (2003). Deforestation and forest degradation factors. Retrieved August 10, 2014, from <http://www.fao.org/docrep/article/wfc/xii/ms12a-e.htm>
- FAO. (2011). *Assessing forest degradation towards the development of globally applicable guidelines*.
- Gabr, S., Ghulam, A., & Kusky, T. (2010). Detecting areas of high-potential gold mineralization using ASTER data. *Ore Geology Reviews*, 38(1-2), 59–69. <http://doi.org/10.1016/j.oregeorev.2010.05.007>
- Gao, Y., Mas, J. F., Niemeyer, I., Marpu, P. R., & Palacio, J. L. (2003). Object-based image analysis for mapping land-cover in a forest area, (8701).
- Ge, L., Chang, H.-C., & Rizos, C. (2007). Mine subsidence monitoring using multi-source satellite SAR images. *Photogrammetric Engineering & Remote Sensing*, 73(3), 259–266. <http://doi.org/10.14358/PERS.73.3.259>
- Geology voice: Potency of gold mineral in Malang Regency (in Indonesia). (2014). Retrieved December 1, 2014, from <http://suarageologi.blogspot.com/2014/05/potensi-mineral-emas-di-kabupaten-malang.html>
- Gibbs, H. K., Brown, S., Niles, J. O., & Foley, J. a. (2007). Monitoring and estimating tropical forest carbon stocks: making REDD a reality. *Environmental Research Letters*, 2(4), 045023. <http://doi.org/10.1088/1748-9326/2/4/045023>
- Hashim, M., Ahmad, S., Johari, M. A., & Pour, A. B. (2013). Automatic lineament extraction in a heavily vegetated region using Landsat Enhanced

- Thematic Mapper (ETM +) imagery. *Advances in Space Research*, 51(5), 874–890. <http://doi.org/10.1016/j.asr.2012.10.004>
- Hedenqulst, J. W., & Lowenstern, J. B. (1994). The role of magmas in the formation of hydrothermal ore deposits.
- Hellman & Schofield Pty Ltd. (2011). *Tujuh Bukit Project Report on Mineral Resources , Technical Report for Interpid Mines Limited*.
- Hidayat, M. Y. (2006). *Evaluation of land suitability of Paraserianthes falcataria L Nielsen in some slope units (case study in Cipatat Bandung West Java) (in Indonesia)*.
- IDL. (2009). ENVI atmospheric correction module: QUAC and FLAASH user's guide. *Module Version*. Retrieved from <http://scholar.google.com/scholar?hl=en&btnG=Search&q=intitle:ENVI+Atmospheric+Correction+Module:+QUAC+and+FLAASH+user's+guide#0>
- Igneous Rocks. (n.d.). Retrieved April 19, 2015, from <http://www.galleries.com/rocks/igneous.htm>
- Indonesia Investments. (2014). Gold mining in Indonesia - Indonesian gold production consumption. Retrieved August 15, 2014, from <http://www.indonesia-investments.com/doing-business/commodities/gold/item167>
- Indonesia Nasional Standard of 7724. (2011). Ground based forest carbon accounting (in Indonesia).
- IPCC. (2006). *Guidelines for national greenhouse gas inventories Volume 4 Agriculture, Forestry and Other Land Use*. Retrieved from <http://www.ipcc-nggip.iges.or.jp/public/2006gl/vol4.html>
- ITT Visual Information Solutions. (n.d.). ENVI Tutorial - Advanced Hyperspectral Analysis.
- Jaya, I. N. . (2006). *Practical guideline of remote sensing*.
- Jordan, G., & Schott, B. (2005). Application of wavelet analysis to the study of spatial pattern of morphotectonic lineaments in digital terrain models. A case study. *Remote Sensing of Environment*, 94, 31–38. <http://doi.org/10.1016/j.rse.2004.08.013>
- Karna, Y. K. (2012). *Mapping above ground carbon using worldview satellite image and lidar data in relationship with tree diversity of forests*. University

of Twente Faculty of Geo-Information and Earth Observation (ITC). Retrieved from http://www.itc.nl/library/papers_2012/msc/nrm/karna.pdf

Kocal, A., Duzgun, H. S., Karpuz, C., Technologies, G. I., Mapping, D., & Imagery, H. (n.d.). Discontinuity mapping with automatic lineament extraction from high resolution satellite imagery.

Kujjo, C. P. (2010). Application of remote sensing for gold exploration in the Nuba Mountains , Sudan, (May).

Lee, J. Y., & Warner, T. A. (2014). Image classification with a region based approach in high spatial resolution imagery.

Li, W., Guo, Q., Jakubowski, M. K., & Kelly, M. (2012). A new method for segmenting individual trees from the Lidar point cloud. *Photogrammetric Engineering and Remote Sensing*, 78, 75–84.

Liu, L., Zhou, J., Jiang, D., Zhuang, D., Mansaray, L. R., & Zhang, B. (2013). Targeting mineral resources with remote sensing and field data in the Xiemisitai area, West Junggar, Xinjiang, China. *Remote Sensing*, 5(7), 3156–3171. <http://doi.org/10.3390/rs5073156>

Lowe, S. (2014). Can mining be part of a low-carbon, low-deforestation development strategy? the case of Guyana. *Environment Magazine*. Retrieved from <http://www.environmentmagazine.org/Archives/Back Issues/2014/May-June 2014/mining-full.html>

Minister of Energy and Mineral Resources. (2014). Decree of Minister of Energy and Mineral Resources No. 1204 K/30/MEM/2014 of mining area in Java and Bali (in Indonesia).

Ministry of Forestry of Republic of Indonesia. Technical guideline of carbon estimation of national forest inventory (in Indonesia) (2013).

Musa, H. D., & Jiya, S. N. (2011). An assessment of mining activities impact on vegetation in bukuru Jos Plateau State Nigeria using Normalized Differential Vegetation Index (NDVI). *Journal of Sustainable Development*, 4(6), 150–159. <http://doi.org/10.5539/jsd.v4n6p150>

Najafi, C. (2011). Gold formation, extraction, and refining in the Sierra Nevada Mountain Region, 1–15.

Natural Gold Indicators (Part 2) | RareGoldNuggets.com. (2014). Retrieved April 14, 2015, from <http://raregoldnuggets.com/blog/?p=750>

- Nguyen, T. N. (2010). *Estimation and mapping of above ground biomass for the assessment and mapping of carbon stocks in tropical forest using SAR data : a case study in Afram headwaters forest, Ghana. University of Twente Faculty of Geo-Information and Earth Observation (ITC)*. Retrieved from <http://adlib.itc.nl/detail.aspx?parentpreref=>
- Patterson, M. E. (2003). Hydrothermal alterations and the formation of metal ores in the Sierra Nevada's. Retrieved April 19, 2015, from <http://www.indiana.edu/~sierra/papers/2003/Patterson.html>
- Perhutani. (2014). *Brief review of illegal gold mining of KPH South Banyuwangi.pdf*.
- Perkins, T., Adler-golden, S., Matthew, M., Berk, A., Anderson, G., Gardner, J., & Felde, G. (2005). Retrieval of atmospheric properties from hyper- and multi-spectral imagery with the FLAASH atmospheric correction algorithm. *Proc. of SPIE Vol 5979 5979E-1*, 5979, 1–11. <http://doi.org/10.1117/12.626526>
- Placer deposit. (2010). Retrieved from <http://www.indiana.edu/~sierra/papers/2010/cross-najafi.html>
- Pour, a B., & Hashim, M. (2014). Alteration mineral mapping using ETM+ and hyperion remote sensing data at Bau Gold Field, Sarawak, Malaysia. *IOP Conference Series: Earth and Environmental Science*, 18, 012149. <http://doi.org/10.1088/1755-1315/18/1/012149>
- Pour, A. B., & Hashim, M. (2014). Hydrothermal alteration mapping using Landsat-8 data, Sar Cheshmeh copper mining district, SE Iran. *Journal of Taibah University for Science*. <http://doi.org/10.1016/j.seizure.2014.02.015>
- Pour, A. B., Hashim, M., & Marghany, M. (2014). Exploration of gold mineralization in a tropical region using Earth Observing-1 (EO1) and JERS-1 SAR data: A case study from Bau gold field, Sarawak, Malaysia. *Arabian Journal of Geosciences*, 7(6), 2393–2406. <http://doi.org/10.1007/s12517-013-0969-3>
- Raina, A. K., & Gupta, M. K. (2009). Soil and vegetation studies in relation to parent material of Garhwal Himalayas, Uttarakhand India.
- Raj, D. P. P. (2005). *Ground improvement techniques (PB)*. Firewall Media. Retrieved from <https://books.google.com/books?id=cDGIhh7ttMcC&pgis=1>
- Ramadan, T. M., & Abdel Fattah, M. F. (2010). Characterization of gold mineralization in Garin Hawal area, Kebbi State, NW Nigeria, using remote

- sensing. *Egyptian Journal of Remote Sensing and Space Science*, 13(2), 153–163. <http://doi.org/10.1016/j.ejrs.2009.08.001>
- Rigina, O. (2002). Environmental impact assessment of the mining and concentration activities in the Kola Peninsula, Russia by multirate remote sensing. *Environmental Monitoring and Assessment*, 75(1), 11–31. Retrieved from <http://www.ncbi.nlm.nih.gov/pubmed/15900663>
- Sabins, F. F. (1999). Remote sensing for mineral exploration. *Ore Geology Reviews*, 14(3-4), 157–183. [http://doi.org/10.1016/S0169-1368\(99\)00007-4](http://doi.org/10.1016/S0169-1368(99)00007-4)
- Sartohadi, J., Sianturi, R. S., Rahmadana, A. D. W., Maritimo, F., Wacano, D., Munawaroh, ... Pratiwi, E. S. (2014). *Landscape of Ijen Volcano and its surrounding*. Yogyakarta.
- Schnitzler, M. (2010). *Calculation of Carbon Capture in Tropical Reforestation Projects La Gamba , Costa Rica (Rainforest of the Austrians)*.
- Shanks III, W. C. P. (2012). *Hydrothermal alteration. Volcanic Massive Sulphide Occurrence Model*.
- Shrestha, S. K. (2011). *Carbon stock estimation using very high resolution satellite imagery and individual crown segmentation (a case study of broadleaved and needle leaved forest of Dolakha , Nepal)*.
- Singh, H., & Huat, B. B. . (2012). *Handbook of tropical residual soils engineering*. CRC Press. Retrieved from <https://books.google.com/books?id=UmWPqahaECIC&pgis=1>
- Sreejesh, K. K., Thomas, T. P., Rugmini, P., Prasanth, K. M., & Kripa, P. K. (2013). Carbon sequestration potential of Teak (*Tectona grandis*) plantations in Kerala, 2, 167–170.
- Sukamar, M., Venkatesan, N., & Babu, C. N. K. (2014). A Review of Various Lineament Detection Techniques for high resolution Satellite Images. *International Journal of Advanced Research in Computer Science and Software Engineering*, 4(3), 72–78.
- Susintowati. (2012). *Mercury bioacumulation and communitystructure of gastropoda in ex-area of traditional gold tailing in Lampon river, Banyuwangi, East Java (in Indonesia)*. Universitas Gadjah Mada. Retrieved from http://etd.ugm.ac.id/index.php?mod=penelitian_detail&sub=PenelitianDetail&act=view&typ=html&buku_id=57729&obyek_id=4

- Tom-Dery, D., Dagben, Z. J., & Cobbina, S. J. (2012). Effect of illegal small-scale mining operations on vegetation cover of arid, 4(6), 674–679.
- Wardani, S. F. Y. (2013). *Estimation of carbon stock changes in above ground woody biomass due to volcano pyroclastic flow and pyroclastic surge : the case of Merapi Volcano National Park. University of Twente Faculty of Geo-Information and Earth Observation (ITC)*. Retrieved from http://www.itc.nl/library/papers_2013/msc/aes/wardani.pdf
- Woldai, T. (2001). Application of remotely sensed data and GIS in assessing the impact of mining activities on the environment, 75–84.
- Woldai, T., & Fabbri, A. G. (1998). The impact of mining on the environment.- a case study from the Tharsis-Lagunazo mining area, Province Huelva, SW Spain.
- Wysocki, D. A., Schoeneberger, P. J., Hirmas, D. R., & LaGarry, H. E. (2011). Geomorphology of soil landscapes. In *Handbook of Soil Sciences* (pp. 1–26). <http://doi.org/doi:10.1201/b11267-35>

LIST OF APPENDICES

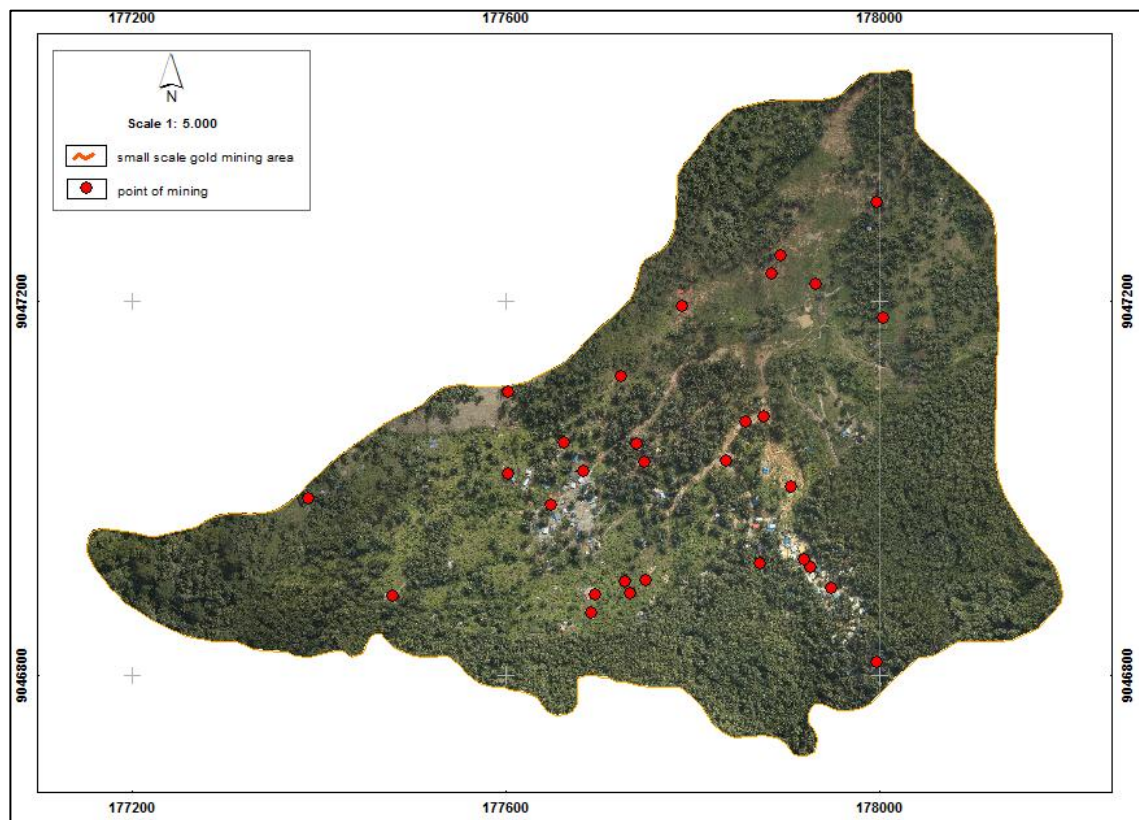
Appendix 1: The performance characteristic of the Landsat-8 sensor

<u>Band Name</u>	<u>Bandwidth (μm)</u>	<u>Resolution (m)</u>
Band 1 Coastal	0.43 – 0.45	30
Band 2 Blue	0.45 – 0.51	30
Band 3 Green	0.53 – 0.59	30
Band 4 Red	0.64 – 0.67	30
Band 5 NIR	0.85 – 0.88	30
Band 6 SWIR 1	1.57 – 1.65	30
Band 7 SWIR 2	2.11 – 2.29	30
Band 8 Pan	0.50 – 0.68	15
Band 9 Cirrus	1.36 – 1.38	30
Band 10 TIRS 1	10.6 – 11.19	100
Band 11 TIRS 2	11.5 – 12.51	100

Appendix 2: Point of gold mining samples

No.	Coordinate		Type	Land cover
	X	Y		
1	177996	9040813	underground	Dense Teak forest
2	177948	9046893	underground	Group of underground mining
3	177925	9046915	underground	Group of underground mining
4	177918	9046923	underground	Group of underground mining
5	177871	9046919	underground	Dense Teak forest
6	177905	9047002	Open mining	river
7	177683	9047018	Open mining	river
8	177648	9046982	Open mining	river
9	177695	9046886	underground	Inactive hole
10	177691	9046867	underground	Inactive hole
11	177893	9047248	underground	Inactive hole
12	177883	9047047	Open mining	river
13	177787	9047192	Open mining	river
14	177661	9047047	Open mining	river
15	177602	9047017	underground	Bare land
16	177479	9046885	underground	Bare land
17	177875	9047076	Open mining	river
18	177855	9047070	Open mining	river
19	177834	9747024	Open mining	river
20	177738	9047047	underground	Medium dense Teak forest
21	177747	9047027	underground	Medium dense Teak forest
22	177749	9046901	underground	Inactive hole
23	177727	9046900	underground	Inactive hole
24	177732	9046887	underground	Inactive hole
25	178003	9047182	underground	Inactive hole
26	177930	9047218	underground	Inactive hole
27	177996	9047305	underground	Medium dense Teak forest
28	177723	9047119	underground	Inactive hole
29	177602	9047102	underground	Bare land
30	177388	9046988	underground	Medium dense Teak forest

Appendix 3: Distribution of mining sample



Appendix 4: Map of Permanent Sample Plot distribution in Indonesia



Appendix 5: Sample data collection sheet

Tally sheet

Name of recorder :		Date :	
Plot number :		X coordinate :	
Slope :		Y coordinate :	
Land cover :		Altitude :	

No.	Species	DBH (cm)	Height (m)	Crown diameter (m)	Coordinate		Remarks
					X	Y	

Appendix 6: Accuracy assessment of DBH-CPA model

<i>Regression Statistics</i>	
Multiple R	0.55
R Square	0.53
Adjusted R Square	0.53
Standard Error	11.11
Observations	96

<i>ANOVA</i>					
	<i>df</i>	<i>SS</i>	<i>MS</i>	<i>F</i>	<i>Significance F</i>
Regression	1	7.32	7.33	23.49	9.9E-11
Residual	95	0.002	0.0003		
Total	96	7.33			

	<i>Coefficients</i>	<i>Standard Error</i>	<i>t Stat</i>	<i>P-value</i>	<i>Lower 95%</i>	<i>Upper 95%</i>
Intercept	1.22	10.54	16.38	1.94E-07	0.16	0.22
X	0.0039	13.45	15.27	3.67E-15	0.29	0.30

Appendix 7: Accuracy assessment of CPA-Carbon model

<i>Regression Statistics</i>	
Multiple R	0.60
R Square	0.53
Adjusted R Square	0.51
Standard Error	7
Observations	96

ANOVA					
	<i>df</i>	<i>SS</i>	<i>MS</i>	<i>F</i>	<i>Significance F</i>
Regression	1	22.79	2.79	23.49	9.9E-11
Residual	95	9.54E-05	1.19E-05		
Total	96	22.80			

	<i>Coefficients</i>	<i>Standard Error</i>	<i>t Stat</i>	<i>P-value</i>	<i>Lower 95%</i>	<i>Upper 95%</i>
Intercept	1.86	5.32	23.23	2.03E-09	1.99	2.07
X	0.013	3.98	43.45	3.13E-08	4.67	5.08

Appendix 8: Communalities of analysis factor

Communalities		
	Initial	Extraction
1	1.000	1.000
2	1.000	.999
3	1.000	.996
4	1.000	1.000
5	1.000	.998
6	1.000	1.000
7	1.000	.998
8	1.000	.952
9	1.000	1.000
10	1.000	1.000
11	1.000	.991
12	1.000	1.000
Extraction Method: Principal Component Analysis.		

Appendix 9: Teak (*Tectona grandis* Sp) conformity land criteria

No	Criteria	Land suitability class			
		S1	S2	S3	N
1.	Average temperature ($^{\circ}\text{C}$)	25-30	30-35	21-25	-
2.	Rainfall (mm)	1500-2000	2000-2250	-	2250-2500
3.	Drainage	good	moderate	slightly bad	bad
4.	Texture	fine, slightly fine, moderate	slightly coarse	coarse	-
5.	Soil thickness (cm)	150	100-150	75-100	50-75
6.	Slope (%)	<8	8-15	15-30	30-50
7.	Acidity level (pH)	5.5-7	7-7.5	7.5-8	-
8.	Risk of erosion	very low	low	moderate	high, very high

Land suitability class is divided into two classes which are suitable (S) and not suitable (N) (Hidayat, 2006). S1 means high suitability of land; which is land does not have minor constraint factor and will not reduce its productivity. S2 means moderate suitability which land has constraint factor that affected the productivity. Therefore, it needs input to overcome the constraint. Meanwhile, S3 means marginal land that has heavy constraint that needs higher input than S2 class. N class is not suitable due to difficult constraint to overcome.

Appendix 10: Field documentation

